

Inventory and GLOF hazard assessment of glacial lakes in the Sikkim Himalayas, India

Nazimul Islam & Priyank Pravin Patel

To cite this article: Nazimul Islam & Priyank Pravin Patel (2021): Inventory and GLOF hazard assessment of glacial lakes in the Sikkim Himalayas, India, Geocarto International, DOI: [10.1080/10106049.2020.1869332](https://doi.org/10.1080/10106049.2020.1869332)

To link to this article: <https://doi.org/10.1080/10106049.2020.1869332>

 View supplementary material [↗](#)

 Published online: 16 Feb 2021.

 Submit your article to this journal [↗](#)

 Article views: 193

 View related articles [↗](#)

 View Crossmark data [↗](#)
CrossMark



Inventory and GLOF hazard assessment of glacial lakes in the Sikkim Himalayas, India

Nazimul Islam^{a,b*}  and Priyank Pravin Patel^c 

^aSchool of Geography, University of Leeds, Leeds, United Kingdom; ^bIndian Institute of Technology, Kharagpur, West Bengal, India; ^cDepartment of Geography, Presidency University, Kolkata, West Bengal, India

ABSTRACT

Glacial Lake Outburst Floods (GLOFs) are a recurring hazard in the Himalayas, posing significant threat to downstream communities. The North Sikkim district of India, comprising the upper reaches of the Teesta River in the Eastern Himalayas, has experienced past GLOF events. The identification of lakes susceptible to this phenomenon is therefore paramount. Using multi-temporal satellite images, this study tracks lake growth in the region, revealing that 203 new lakes had developed herein during the observation period (2000–2018). Of these, 82 lakes had formed during 2011–2018 alone; indicating marked glacial retreat and consequent lake area growth, alongside a rising temperature trend. Using various weighted geometric and geomorphic parameters, the 36 most hazardous lakes were identified, from which the 10 lakes posing the greatest GLOF threat were discerned. These lakes are mostly situated along the main snowline and Great Himalayan water-divide in the north-eastern part of Sikkim and should be monitored continuously.

ARTICLE HISTORY

Received 11 September 2020
Accepted 5 December 2020

KEYWORDS

Eastern Himalayas; GLOF; glacier; glacial lake; lake mapping

1. Introduction

The Himalayas possess one of the largest sources of snow and ice outside the Polar Regions (SAC (Space Application Centre) 2016), with an estimated glacier coverage of 60,000 km² (Kääb et al. 2012). However, Himalayan glaciers are presently losing an average of about 0.4% of their mass per year (Chand and Sharma 2015) and have already reduced or are expected to decrease significantly over the coming decades (Bohner and Lehmkühl 2005; Bajracharya et al. 2007; Bolch et al. 2012; Wiltshire 2014; Zhao et al. 2014; King et al. 2017), due to an estimated temperature increase between 1 °C and 6 °C in the region (IPCC 2007). While glacier mass and related glacial lake area changes have been comparatively well documented in the western part of the Indian Himalayas (e.g. Kulkarni et al. 2011), comparatively lesser information is available for its eastern section, of which the Sikkim Himalayas is a part (Basnett et al. 2013), even though there have

CONTACT Priyank Pravin Patel  priyank999@hotmail.com

*Present address: Institute of Earth Surface Dynamics (IDYST), University of Lausanne, Switzerland.

 Supplemental data for this article is available at <https://doi.org/10.1080/10106049.2020.1869332>.

© 2021 Informa UK Limited, trading as Taylor & Francis Group

been a number of recent studies specific to this area (e.g. Frey et al. 2014; Racoviteanu et al. 2015; Hazra and Krishna 2019).

The Sikkim Himalayas (the focus of the present study), too has experienced similar rapid changes in glacier coverage (Quincey et al. 2007; Khadka et al. 2018). About 200 km² of glacial area has been lost in its Teesta River Basin between 1990 and 2010, leading to the formation of a large number of debris covered supraglacial and moraine dammed lakes (Basnett et al. 2013). This is evident by the large number of glacial lakes that have appeared herein and across the rest of the Himalayas (Zhang et al. 2015; Aggarwal et al. 2016; Nie et al. 2017; Khadka et al. 2018, 2019), with their volumes being steadily augmented by further glacial retreat (Mool et al. 2001). Aggarwal et al. (2016) and Campbell (2005) have respectively mapped 143 and 266 glacial lakes in the Sikkim region and a rise in the number of glacial lakes creates the prospect of multiple, hazardous Glacial Lake Outburst Flood (GLOF) events that occur when a large volume of water is suddenly released from them (Clague and O'Connor 2015; Veh et al. 2020). GLOFs are of a flash flood nature, being rapid and catastrophic occurrences (Kron 2005), and are usually triggered by avalanches/mass movements, intense rainfall/cloudbursts or seismic events (Richardson and Reynolds 2000; Emmer and Cochachin 2013; Aggarwal et al. 2017; Debnath et al. 2018). The high glacial area shrinkage in the Himalayas (and especially the breaking up and retreat of large glaciers), can enable the formation/expansion of numerous glacial lakes, thereby increasing the susceptibility of this region to GLOF events (Veh et al. 2020).

Glacier retreat has long been recognized as a major problem in the Indian Himalayan region, including in the Sikkim Himalayas (NRC, 2012). Retreat rates estimated for 1868 glaciers from 11 Himalayan basins, by examining their respective changes since 1962, have revealed an overall deglaciation of 16% (Kulkarni et al. 2011). The retreating of glaciers causes meltwater to accumulate in front of the calving and thawing glacial snout and such lakes would eventually burst forth (Clague and O'Connor 2015) in episodic high-intensity events. With continued glacial retreat and mass loss, spring thaw volumes would diminish (Milner et al. 2017) and make downstream reaches susceptible to droughts (NRC, 2012; Immerzeel et al. 2020), while episodic GLOF events could still occur in upstream valley sections from accumulating meltwaters. Therefore glacial retreat shall have complex impacts on stream hydrographs (Milner et al. 2017).

However, only a few studies have quantified the glacial mass balance for the purpose of GLOF analysis in the Sikkim Himalayas (e.g. Basnett et al. 2013; Worni et al. 2013; Raj et al. 2013a; Debnath et al. 2018; Dubey and Goyal 2020) and studies on the glacial surface changes occurring across different glacial size classes are less in number (e.g. Frey et al. 2014; Racoviteanu et al. 2015; Shukla et al. 2018; Debnath et al. 2019; Hazra and Krishna 2019). The number of glacial lakes has risen rapidly in this region (Shukla et al. 2018) and several inventory studies have been undertaken recently in Sikkim and its neighbouring Himalayan areas of Nepal and Bhutan (e.g. Rounce et al. 2017; Khadka et al. 2018, 2019; King et al. 2018; Tsutaki et al. 2019; Maskey et al. 2020). For example, Hakeem et al. (2018) documented the presence of 301, 302 and 644 glacial lakes in 2000, 2007 and 2014, respectively, clearly denoting the marked growth in lake numbers. A similar study by Raj et al. (2013b) had previously identified the formation of 85 new lakes in this region, with overall numbers rising from 266 in 2003 to 320 in 2010, of which 14 lakes were identified as being most susceptible to GLOF events based on their areal extents/changes. Aggarwal et al. (2017) demarcated 1104 glacial lakes in the Sikkim Himalayas, of which 21 were identified as being susceptible to GLOF events using the Weighted Index Overlay and Analytic Hierarchy Process approach. An in situ GPS-and-bathymetric survey for assessing the growth of the

South Lhonak Glacial Lake in the Upper Teesta Basin has revealed an average areal expansion of 0.03 km^2 per year (Sharma et al. 2018). The same lake has also been physically modelled to envisage moraine dam breaching scenarios leading to GLOFs (Begam et al. 2018), while Schwanghart et al. (2016) have estimated the threat posed to downstream hydroelectric power projects by such events.

In the above context, many researchers (e.g. Rowan et al. 2015; Zhang et al. 2019) have emphasized the importance of preparing updated glacial lake inventories for gauging the GLOF susceptibility in the Himalayan region. Usually, multi-temporal and multi-spectral satellite images (mostly from the Landsat series – Yan et al. 2017; Veh et al. 2018) and the Google Earth platform have been used for this purpose. The results derived from such analyses are however comparable with findings elicited from higher resolution datasets (Mir et al. 2018; Zhang et al. 2018). Such repeat-surveys are required for inventorying glacial lakes at regular intervals to keep track of their changing environmental conditions and GLOF hazard status (Nie et al. 2017, 2018). For example, Begam and Sen (2019) used repeat survey satellite images for delineating moraine dammed glacial lakes in the Central and Eastern Himalayas, showing how lakes therein had expanded by an astonishing 43.6% during 1990–2015, and related their expansion rates with the probability of a GLOF event. A similar study in the Koshi Basin in the Central Himalayas, adjacent to Sikkim, documented that from 1977 to 2010 the number of glacial lakes had increased by 86.9% and that their cumulative area had also increased by 35.1% (Shrestha et al. 2017).

This study is thus pertinent in seeking to map and create an inventory of such newly formed glacial lakes in part of the Sikkim Himalayas as well as document those that have notably enlarged in terms of their area. In doing so, we provide one of the most recent updated high-resolution inventories of glacial lakes in this region. Furthermore, we shall gauge which of these lakes are presently most susceptible to a GLOF event on the basis of the recent expansion extents and ambient characteristics. This can serve as a prior indication to monitor them closely.

2. Objectives

In keeping with the foregoing discussion, this study aims to:

- i. Create an updated glacial lake inventory of a part of the Sikkim Himalayas using multi-temporal satellite images (for the years 2000, 2008, 2011 and 2018) of medium to high resolution,
- ii. Identify potentially hazardous lakes that may be prone to GLOF events, and
- iii. Analyze the pertinent climatic variables (mean temperature and annual rainfall) in the long term and also focussing on the time period of 1990 to 2015, for comparing their trends with the ambient glacial lake dynamics.

3. The study area

The eastern Himalayan state of Sikkim ($27^{\circ}22'41.3''\text{N}$ to $28^{\circ}07'50.5''\text{N}$ and $88^{\circ}06'59.8''\text{E}$ to $88^{\circ}53'41''\text{E}$) in India shares international borders with China (in the north and north-east), Bhutan (southeast) and Nepal (west). It extends 81.5 km from north to south and 70 km from east to west, with a total geographical area of 4263.7 km^2 (Figure 1). According to the Indian Census of 2011, its four districts (North, South, East and West Sikkim) together have a total population of 610,577. The state is poorly connected and North Sikkim District ($27^{\circ}22'41.1''\text{N}$ to $28^{\circ}07'50.5''\text{N}$ and $88^{\circ}07'02.0''\text{E}$ to $88^{\circ}53'37''\text{E}$) is

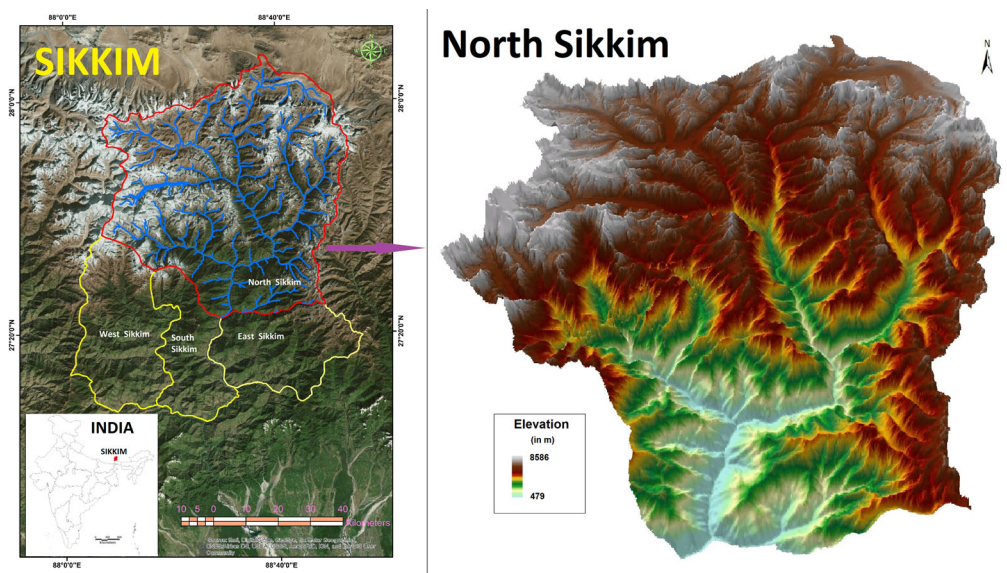


Figure 1. Location of the study area (North Sikkim District) in India.

mostly inaccessible (being traversed north to south by the National Highway No. 31 A – the only major road in the region), due to its rugged topography. This district is the focus of the present study due to its preponderance of glaciers and glacial lakes. The mean annual temperature of North Sikkim is 18 °C and the annual rainfall received varies from 127 to 508 cm (as measured during 1990–2015 from the gridded India Meteorological Department (IMD) dataset of the area). Dense forests and snow covered regions predominate and constitute four ecological zones, viz. subtropical, temperate, sub-alpine and alpine (Rai et al. 2000). The mountain ranges are mostly comprised of gneiss and schist (Geological Survey of India (GSI) 2012) and the combined effects of heavy rainfall, structural weaknesses and steep slopes make them highly susceptible to denudation (Mehrotra et al. 1996).

The Teesta (or Tista), a right bank tributary of the mighty River Brahmaputra, originates from the Phunri Glacier at an elevation of 7127 m. The upper reaches of its basin, which comprises the entire territory of the North Sikkim district, is vulnerable to a range of natural hazards (Mandal and Chakrabarty 2016), like earthquakes, rockfalls and landslides along with cloudbursts, flash floods and GLOFs (Ramakrishnan et al. 2005; Nath et al. 2008; Pal et al. 2008; Sharma et al. 2014; Gupta et al. 2015; Mandal and Chakrabarty 2016; Kumar et al. 2018; Sattar et al. 2019). This area has also experienced a notable decline in its glacial coverage (SAC 2016), resulting in the formation of a number of lakes at high altitude, which therefore manifest a persistent GLOF threat.

4. Datasets and methods

4.1. Datasets used

A number of datasets have been used in this study. Initially, Survey of India topographic maps at 1:250,000 scale were used to demarcate the borders of North Sikkim district. Thereafter, different sets of satellite images for the four time periods examined were procured for creating used to create the glacial lake inventory (Table 1). As part of this, the

Table 1. Details of satellite image and DEM datasets used in the study.

Satellite Sensor	Row	Path	Date of Acquisition	No of Scenes used	Resolution		
					Spectral (μm)	Spatial (m)	Temporal (days)
Landsat 7 ETM+	41	139	26 Dec 2000	01	B1: 0.45–0.52 (Blue) B2: 0.52–0.60 (Green) B3: 0.63–0.69 (Red) B4: 0.76–0.90 (NIR) B5: 1.55–1.75 (SWIR) B6: 10.40–12.50 (TIR) B7: 2.08–2.35 (SWIR)	30	16
ResourceSat-1 LISS-III	51	107	17 Dec 2008	3	B2: 0.52–0.59 (Green)	23.5	24
	52	107	17 Dec 2008	12	B3: 0.62–0.68 (Red) B4: 0.77–0.86 (NIR) B5: 1.55–1.70 (SWIR)		
ResourceSat-1 LISS-IV MX	52	107	20 Nov 2011	01	B2: 0.52–0.59 (Green) B3: 0.62–0.68 (Red) B4: 0.77–0.86 (NIR)	5.8	24
ResourceSat-2 LISS-IV MX	52	107	23 Jan 2018	01	B2: 0.52–0.59 (Green) B3: 0.62–0.68 (Red) B4: 0.77–0.86 (NIR)	5.8	24
Alos-Palsar DEM by-product	504	530	24 Mar 2008	01	Panchromatic Single Band data (L Band)	12.5	46
	504	540	24 Mar 2008	01			
	504	550	24 Mar 2008	01			
	505	540	11 Apr 2008	01			

Source: Prepared by the authors.

respective high and medium spatial resolution multi-spectral ResourceSat-1 and ResourceSat-2 LISS-IV MX (5.8 m) and LISS-III (23.5 m) scenes were obtained from the National Remote Sensing Centre (NRSC), India. The older and relatively coarser spatial resolution Landsat-7 Enhanced Thematic Mapper (ETM+) scenes (30 m) were downloaded from the United States Geological Survey (USGS) data repository. For ascertaining the terrain attributes and extracting stream networks, the relevant tiles of the Alos Palsar Digital Elevation Model (DEM) by-product of 12.5 m resolution were procured from the European Space Agency (ESA) data portal. Long-term temperature and rainfall data (1901–2002) were obtained from the India Water Portal (https://www.indiawaterportal.org/met_data/) that disseminates such information collated from the IMD database, which can be used for a range of climatic and related hazard analysis (e.g. Thomson 2014; Sahana and Patel 2019). For a more recent insight into these two parameters, gridded temperature and rainfall data at 1° interval (product nos. 3/2008 and 1/2005 respectively – tile centre at 27°50'00"N and 88°50'00"E in North Sikkim district) for 26 years, from 1990 to 2015, was obtained from the IMD for analyzing their respective trends. The relevant seismicity data was obtained from the USGS earthquake data repository (<https://www.usgs.gov/natural-hazards/earthquake-hazards/earthquakes>).

4.2. Data processing tools

Erdas Imagine 2016 was used for pre-processing and sharpening of the raw satellite images and for preparation of the land use and land cover (LULC) layer through

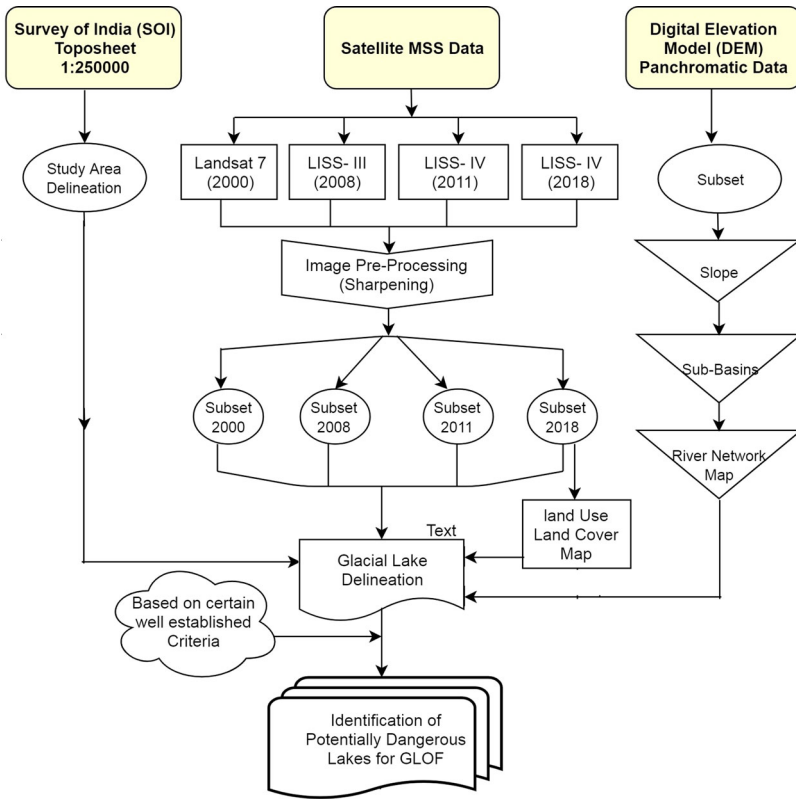


Figure 2. Flowchart of the workflow process.

maximum likelihood (MXL) supervised classification. It was also used for extracting the Normalized Difference Snow Index (NDSI), which is defined as the normalized difference of one visible band and one near-infra-red or short-wave infra-red band (Hall and Riggs 2014). The NDSI was computed, following Hazra and Krishna (2019) as

$$\text{NDSI} = (\text{Green Band} - \text{SWIR Band}) / (\text{Green Band} + \text{SWIR Band}) \quad (1)$$

The NDSI parameter has been used in a number of previous studies to facilitate glacial lake delineation and glacier mapping (e.g. Rathore 2018; Li et al. 2019; Zhang et al. 2019; Yan et al. 2020). We chose to use the NDSI and not another commonly used parameter like the Normalized Difference Water Index (NDWI) (cf. Huggel et al. 2002; Shukla et al. 2018; Begam and Sen 2019), since there was considerable snow/ice cover over many lakes and thus these would not get properly extracted through the NDWI as their spectral reflectance would vary from that of open water bodies. ArcGIS 10.4.1 was used as the main platform for glacial lake delineation and the subsequent geospatial analysis. QGIS 2.14.6 was used for obtaining the elevation profile required for calculating the slope differences from the glacier snout to the lake outlet point, this being one of the required parameters for identifying lakes that are susceptible to GLOF events (see Section 4.5). The extracted annual rainfall and mean temperature values from the IMD datasets were plotted in respective climatic diagrams using MS-Excel. Trend analysis of the temperature datasets was performed via the non-parametric Mann-Kendall test (Kendall 1975; Gilbert 1987) using the XLSTAT extension (https://help.xlstat.com/s/article/mann-kendall-trend-test-in-excel-tutorial?language=en_US) for MS-Excel (cf. Karmeshu 2012).

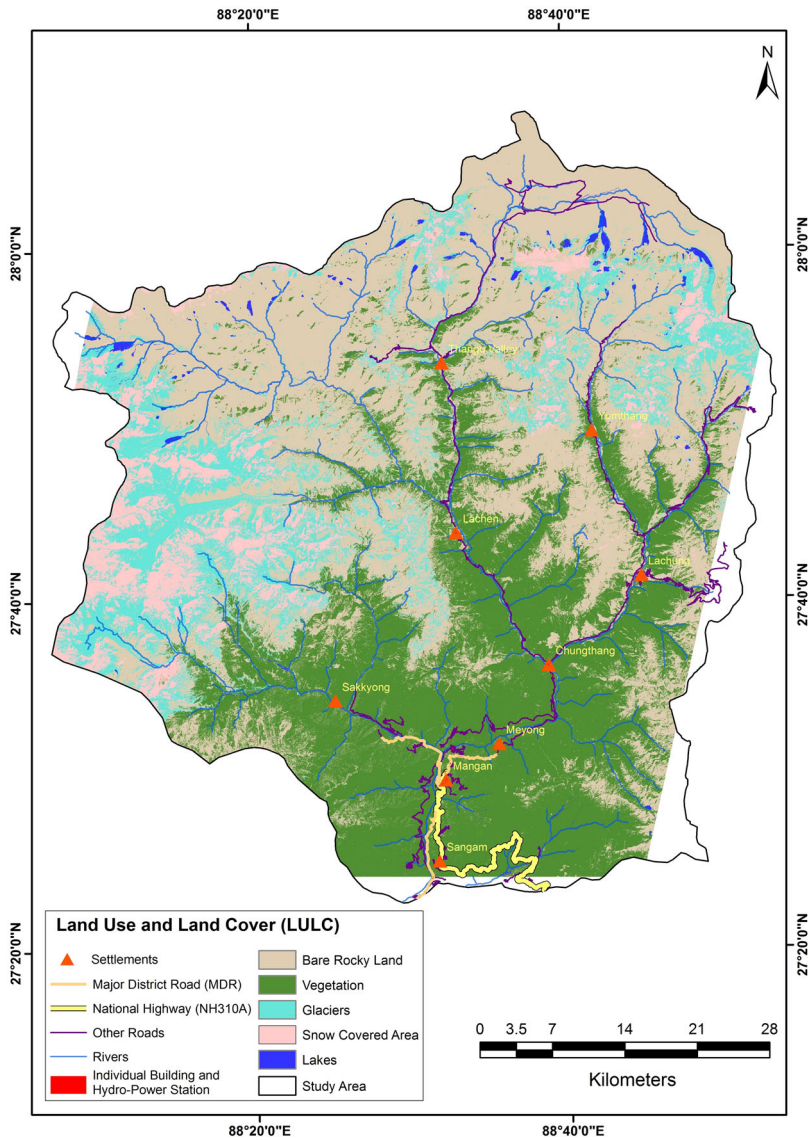


Figure 3. Land use and land cover map of North Sikkim (based on ResourceSat-2 LISS-IV MX images of January 2018).

4.3. Image and DEM analysis

Figure 2 encapsulates the entire workflow for delineating the respective glacial lake dimensions for the various years and the eventual assessment of their GLOF hazard status. The LULC map (Figure 3), prepared from the most recent satellite image dataset (from 5.8 m resolution LISS IV-MX images of January, 2018) based on level one classification scheme (Anderson et al. 1976), comprised of five classes, viz. bare rocky lands, vegetation cover, glaciers, snow cover and water bodies (mainly lakes). Due to complexities in the land cover and a similar spectral reflectance, agricultural land (mostly comprising of terraced plots on steep slopes) could not be distinguished from natural vegetation. Snow cover dominated the study area comprising 38% (or 1620.3 km²) of the landscape,

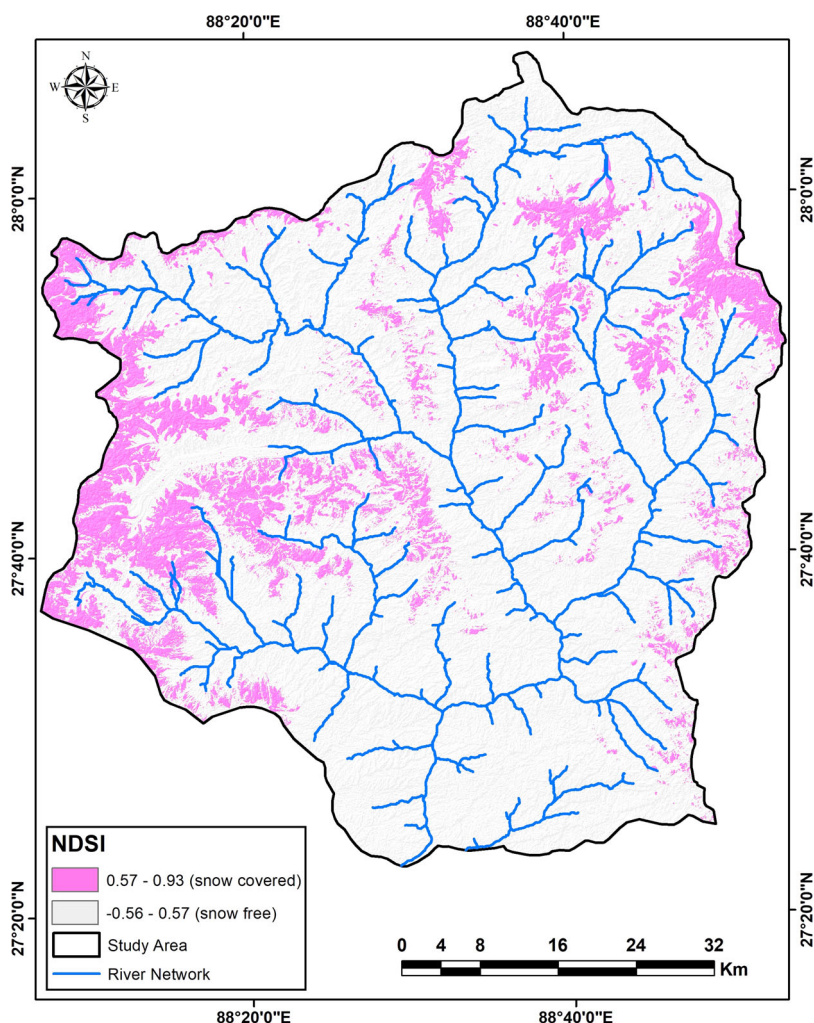


Figure 4. Normalized Difference Snow Index Map of North Sikkim.

followed by vegetation (27.7%), bare rocky lands (21.6%), glacial cover (12.3%) and water bodies (0.3%). A certain small portion (3.2%) remained unclassified due to the unavailability of this high-resolution image dataset for that part. The prepared LULC map was used as an initial determinant of the various snow-covered/glacial regions in the study area. It was also used to discern other water bodies that could be glacial lakes, which could then be examined further through on-screen visualization/digitization. The extracted NDSI layer (Figure 4) was used to cross-check the accuracy of the delineated glacial zones before proceeding for further analysis. The slope map was extracted from the DEM dataset using the relevant tools present in ArcGIS. The stream network of the area was demarcated as per the Strahler (1957) stream ordering method, following the standard procedures of flow routing, flow accumulation and drainage line extraction (e.g. Patel and Sarkar 2009, 2010; Patel 2013). From the obtained stream network layer, four sub-basins, viz. Upper Teesta (UT), Lachung Chhu (LC), Tolung Chhu (TC) and Central Teesta (CT) were delineated.

4.4. Glacial lake delineation, coding and measurements

Once the above snow/glacier zones and sub-basins were obtained, glacial lakes for the different time periods were manually delineated from the respective sharpened images (image filtering was done using a 3×3 sharpening filter) using the polygon and stream-line digitization technique in ArcGIS. These were verified using the higher resolution Google Earth images. A unique code (e.g. 'EHS_UT_015') was assigned to each lake, where EHS denoted Eastern Himalayan Sikkim, 'UT' referred to Upper Teesta and the last three characters (015) were that lake's sequential number. The lakes present in the 2018 dataset were coded first in this manner. If these lakes were also present in the previous years' datasets, the respective codes were transferred to the corresponding features; else suitable codes were assigned afresh. This was done repeatedly till all the lakes in each of the four years were assigned their respective codes. The area and perimeter parameters for each lake were extracted directly from the ArcGIS software domain using the relevant measuring tools, once the glacial lake delineation was complete. To compute the lake depth and volume, the empirical equations developed by Huggel et al. (2002) were used:

$$V = 0.104 * A^{1.42} \quad (2)$$

$$D = 0.104 * A^{0.42} \quad (3)$$

where V and D stood for the lake volume (in m^3) and depth (in m), respectively, and A was the lake area (in m^2). By examining the dimensions of the common lakes that were present in each of the four time periods, further insights were obtained into their growth/shrinkage dynamics in this region.

Apart from using high-resolution Google Earth images to visually verify the glacial lakes delineated, uncertainty calculations were also undertaken to substantiate the veracity of the four datasets derived, especially the accuracy of the obtained lake area. Conventionally, half or one pixel is taken as the linear resolution error, assuming that, on average, the lake margin passes through the centre of the pixels situated along its perimeter (Salerno et al. 2012). We computed the uncertainty following standard methods in the literature (e.g. Gardelle et al. 2011; Wang et al. 2012; Debnath et al. 2018; Shukla et al. 2018; Begam and Sen 2019), by comparing individual lake objects with the image pixels from which they had been extracted. The formula used for computing this was [after Salerno et al. (2012) and Basnett et al. (2013)]:

$$U = \left(\frac{N}{2} \right) \times A \quad (4)$$

where U denoted the uncertainty for a particular lake, N was the number of pixels counted along that lake's perimeter and A was the area covered by a pixel in the image used to extract/digitize that lake. The obtained uncertainty value for each lake was converted into the uncertainty percentage for that lake based on its area derived after digitization.

4.5. Identification of potentially dangerous glacial lakes

The most recent high-resolution dataset available (ResourceSat-2 LISS-IV MX images of January 2018), was used to identify those lakes from which GLOFs were likely to occur. The various geometrical (e.g. related to the lake dimensions) and geomorphic parameters (e.g. related to the ambient/surrounding topographic attributes) commonly used to categorize the GLOF susceptibility status are well documented in the literature (e.g.

McKillop and Clague 2007; Westoby et al. 2014; Prakash and Nagarajan 2017; Allen et al. 2019). We chose similar parameters, based on the available data for this area and following the recommendations of the Glacier and Permafrost Hazards in High Mountains (GAPHAZ) scheme (Allen et al. 2017). The GAPHAZ framework categorizes the hazard assessment variables for a GLOF event under different heads – Atmospheric, Cryospheric and Geotechnical and Geomorphic. Since information about all the variables listed in the scheme was not available, selected parameters were chosen under each head. These were:

- i. Size of the lake (i.e. its area): Larger lakes are expectedly more likely to cause a GLOF event (Iribarren et al. 2014).
- ii. Expansion in lake area since 2011: Lakes that had enlarged markedly since 2011 were considered to be potentially dangerous in GLOF terms (e.g. Bolch et al. 2011). If a lake was non-existent in 2011 (i.e. had newly formed in 2018 or may not have been detected due to extensive snow cover obscuring it), then the lowest weight was assigned (so that while this factor was at least considered in the ensuing analysis, its import was not overestimated).
- iii. Slope difference from glacier snout to the lake outlet: A higher slope difference between the glacier snout and lake outlet would be more likely to induce the lake to overflow its bounds (Wang et al. 2011).
- iv. Connection or proximity with parent glacier and river channel: The connection of each lake, on one side with its parent glacier and on the other with a river channel, provides a ready path for rapid and substantial discharge during a GLOF event (Wang et al. 2011).
- v. Availability of rocks surrounding the lake (for rockfalls and avalanches): The presence/accumulation of debris (rocks or boulders) or steep scarps around a lake is crucial to its hazard status, since mass movements into a lake can cause it to overflow (Huggel et al. 2004; Allen et al. 2019).
- vi. Lake distance from the basin outlet point: Lakes located far away from the basin outlet are less likely to pose substantial threat to their most downstream reaches, as longer GLOF paths would lessen its impact at the basin mouth and vice-versa (Wang et al. 2011).
- vii. Height of the lake outlet dam: Lower dams (usually of moraine deposits) obviously have higher probabilities of getting breached (Huggel et al. 2004). The conditions around each lake were gauged through visual interpretation of the satellite images (LISS-IV/Google Earth) and the discernable dam height was extracted from the DEM dataset. We desisted from incorporating additional parameters about the moraine dam geometry (e.g. Huggel et al. 2004; Prakash and Nagarajan 2017), to avoid overstating this aspect in the ensuing analysis. Furthermore, being loosely consolidated, sinuous/curvilinear features, such dams would be unlikely to have the same dimensions everywhere and dam breaching/slumping/seepage is possible at each spot, which can then spread quickly along the feature. Thus only its height was considered as any dam's primary dimension.

While we did note the seismicity in the region, we did not include this parameter directly in the analysis (e.g. Mergili and Schneider 2011; Prakash and Nagarajan 2017) since proximity to historical earthquake epicentres does not necessarily guarantee future large quakes and mass movements in this region can also be triggered by higher magnitude seismic events occurring afar. The seismicity map prepared has simply been used as an indicator of possible such events in North Sikkim.

Weights to individual parameters (Table 2) were assigned following Huggel et al. (2002) by adopting a scaling norm of 1–3 (where, 1 was the minimum and 3 was the maximum weightage accorded). We opted for utilizing the same range and strength of weights for each of the parameters, as per Huggel et al. (2002), instead of following a differentially weighted approach (e.g. Aggarwal et al. 2017; Prakash and Nagarajan 2017), in order to avoid any user bias while formulating the latter. The Cumulative Weight (CW) of each lake was derived from the summation of the weights given to the individual parameters. The respective lake CWs were finally classified as denoting High ($CW \geq 16$), Medium (CW ranging from 13 to 15) or Low ($CW \leq 12$) Hazard status, in respect of how feasible it was that a GLOF event could be triggered by/from them. Though the lake volume and depth had been estimated, these parameters were not included in the above list to avoid autocorrelation during the ensuing analysis, since they were derived from the lake size parameter.

5. Results and discussion

5.1. Glacial lakes inventory

Glacial lakes inventoried for the years 2000, 2008, 2011 and 2018 in North Sikkim numbered 151 (total area 18.4 km²), 179 (total area 19.7 km²), 272 (total area 19.8 km²) and 354 (total area 25.3 km²), respectively (Figure 5, Table 3). Notably, 203 new lakes were demarcated in the 2018 dataset which were not there in the year 2000 and the overall lake area increased by 6.9 km² during the same period (a rise of 37.5%). In all, 85 lakes were found to be present in all the four time periods examined, with two such lakes present in the Central Teesta sub-basin, 17 in Lachung Chhu, four in Tolung Chuu and 62 lakes in the Upper Teesta sub-basin (for details see Supplementary Information Table S1). Thus, Lachung Chuu and Upper Teesta sub-basins contained the most number of lakes that were present (or common) in the entire study period. Examination of the respective areas of these common lakes revealed that there had been a slight to marked overall increase in almost every lake's area from 2000 to 2018. Those that did not increase in size notably, usually retained their previous dimensions from the year 2000, while only a few lakes showed any perceptible areal decline. The lake area had remained quite constant for the few common lakes present in the other two sub-basins.

The significant increase in the total number of glacial lakes and their overall areal increase in the more recent inventories may have arisen from the use of higher resolution (5.8 m) images to create the 2018 and 2011 databases in comparison to the medium resolution (23.5 and 30 m, respectively) images of 2008 and 2000, by allowing more smaller lakes to be detected. Most of these new lakes were located in the Upper Teesta sub-basin (Figure 6). However, comparison of the 2011 and 2018 datasets (both extracted from similar 5.8 m resolution images), revealed that the number of glacial lakes had indeed increased quite markedly across the entire study area, especially in the Lachung Chuu sub-basin. Similarly, comparison of the respective areas of the common lakes present in the 2018 and 2011 datasets (a total of 169 lakes, with two lakes in the Central Teesta region, 39 in Lachung Chhu, nine in Tolung Chuu and 119 lakes in the Upper Teesta region) shows a marked increase in the dimensions of many lakes. In the Lachung Chuu and Upper Teesta regions (these two zones having the most lakes), their net area increased by about 0.62 and 2.1 km², respectively, with 11 lakes recording a more than 100% areal increase during the same time period while the extents of nine other lakes rose by 30–100% of their former size (see Supplementary Information Table S2). Overall,



Table 2. Weights assigned to the different parameters for GLOF hazard assessment.

Parameter	Range (in km ²)	Weight	Parameter	Range (in °)	Weight	Parameter	Range (in m)	Weight	Parameter	Range (in m)	Weight
Change in lake area	0.1-0.5	3	Slope difference between glacial snout and lake outlet	> 20	3	Connection / Proximity to Parent Glacier	Connected	3	Connection with river channel	Connected	3
	0.009-0.1000	2		10-20	2		Not connected	2		Not connected	2
Height of Dam	< 0.009 or area increased or NA	1		0-10	1		Not in proximity to a glacier	1		Not in proximity to a river channel linkage	1
Height of Dam	< 20	3	Availability of rocks for avalanches / rockfall	Yes	2	Distance from the Basin outlet	< 50	3			
	20-50	2		No	1		50-70	2			
	> 50	1			1		> 70	1			

Source: Prepared by authors based on Huggel et al. (2002).

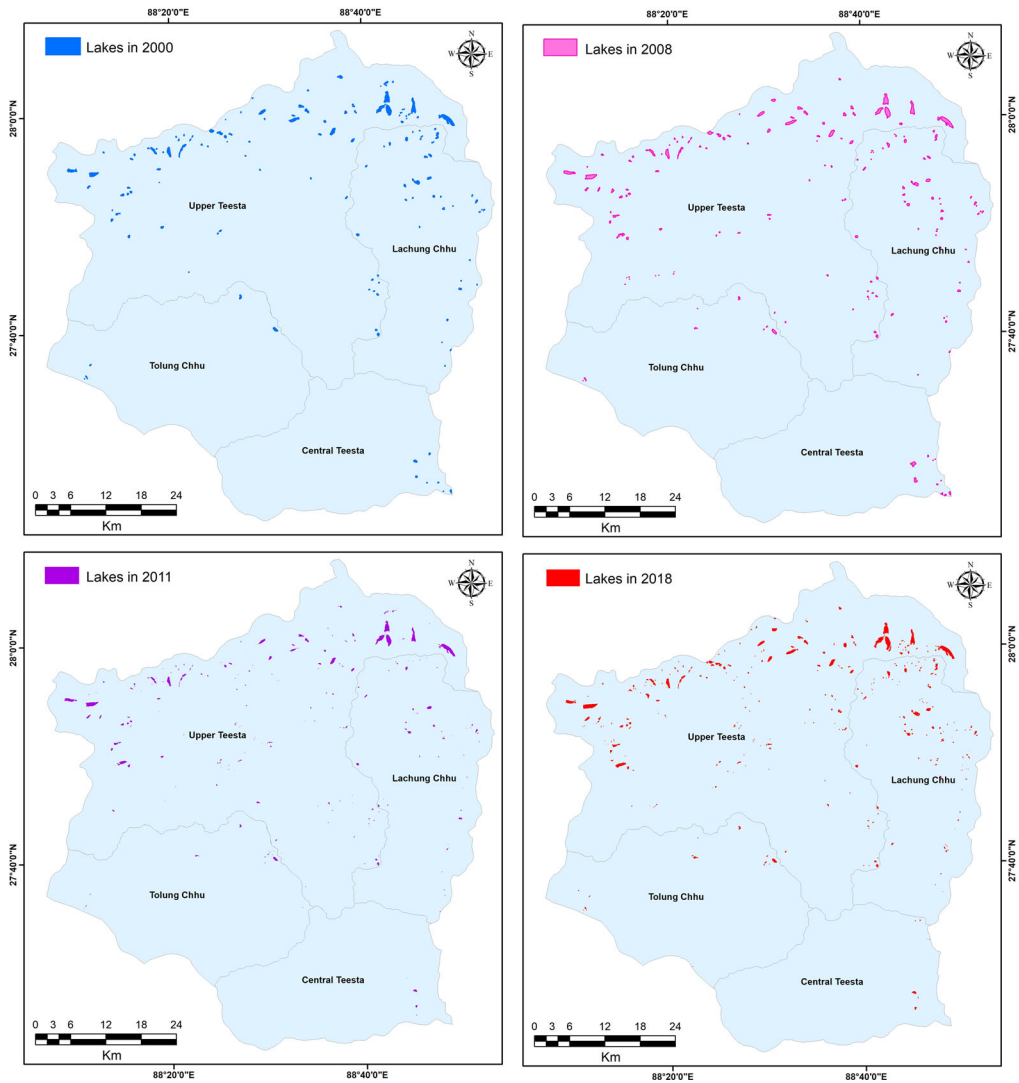


Figure 5. Glacial lakes delineated in North Sikkim in the different years.

from 2000 to 2018, the total lake area in North Sikkim increased by 2.8 km^2 – a substantial rise of 15.65%. All of this points towards an enhanced GLOF susceptibility herein. As the Upper Teesta sub-basin contains about 60% of all glacial lakes in North Sikkim in the most recent inventory and this figure rises to 93.5% when the Lachung Chhu sub-basin is also included, these two regions assumed the most importance during the ensuing GLOF susceptibility analysis.

Since the number and size of glacial lakes had increased tremendously since 2000, further classifications were done based on the respective lake dimensions (area, perimeter, volume and depth) for each sub-region. Results reveal that smaller (lake area $< 10,000 \text{ m}^2$) and medium-sized lakes had increased rapidly (in both number and areal extent), as compared to the larger lakes (lake area $> 500,000 \text{ m}^2$). A summary of the lake inventories based on lake size (Table 4), depth (Table 5) and volume (Table 6), reveals the region-wise variations in lake numbers as per these dimensions from 2000 to 2018

Table 3. Sub-basin wise distribution of glacial lakes and their areal coverage in the different time periods.

Sub-basins	Sub-basin area (km ²)	2000			2008			2011			2018		
		No	Total area (km ²)	Average area (km ²)	No	Total area (km ²)	Average area (km ²)	No	Total area (km ²)	Average area (km ²)	No	Total area (km ²)	Average area (km ²)
Upper Teesta	2079.66	99	14.44	0.15	106	14.77	0.14	200	16.65	0.08	215	20.04	0.09
Lachung Chhu	826.495	40	2.87	0.07	54	3.24	0.06	49	2.16	0.04	116	4.08	0.04
Tolung Chhu	848.795	5	0.57	0.11	8	0.62	0.08	19	0.62	0.03	16	0.84	0.05
Central Teesta	698.274	7	0.51	0.07	11	1.05	0.10	4	0.32	0.08	7	0.36	0.05
Total	4453.224	151	18.39	0.07	179	19.69	0.10	272	19.76	0.08	354	25.33	0.05

Source: Prepared by authors on basis of analysis of satellite images.

(for further details see [Supplementary Information Tables S3–S6](#)). The rise in lake numbers across all size ranges is clearly discernable, with a greater increase in the number of smaller lakes, most of which have been newly formed from the ongoing glacial melt in the region, as was similarly inferred by Hakeem et al. (2018) and Raj et al. (2013a, 2013b). Especially in the Upper Teesta sub-basin, the number/total area or both have increased for lakes of all size classes during the entire study period. Marked changes in lake numbers have occurred in the Lachung Chhu area, which had no lakes smaller than 10,000 m² in 2000 but reported 56 such lakes in 2018, while its lake numbers in the 10,000–50,000 m² class had nearly doubled from 22 in 2000 to 41 in 2018. Even accounting for a greater number of smaller lakes probably being detected from the higher resolution images used to create the more recent inventories, it was still notable that the lake numbers for Lachung Chhu in the aforementioned two size classes had respectively increased from 13 to 56 and 24 to 41 during 2011 to 2018 (both these databases being derived from 5.8 m resolution images). Therefore, the rise in lake numbers and their overall expansion has been unmistakable in the region. In the inventories of 2011 and 2018, a notable increase in the total lake perimeter has also been detected. A greater lake perimeter offers a larger distance through which a possible breach can occur, more so if the mean perimeter of the larger lakes increase, as was noted in the Upper Teesta sub-basin. Smaller and shallower glacial lakes predominate, with 270 out of 354 lakes in the 2018 dataset recording depths of ≤ 10 m. With the rise in lake numbers, their total volume has also risen. Of particular concern is the increase in the total number, area and volume of the largest lakes, which are more prone to a GLOF event.

5.2. Uncertainty analysis for the demarcated glacial lake extents

The percentage uncertainty computed for the individual lakes was classified as per the lake area extents (following [Table 4](#)) to obtain a more meaningful insight into the accuracy levels of the four datasets ([Table 7](#)), following similar approaches adopted by Shukla et al. (2018) and Begam and Sen (2019). The image resolution obviously had an impact on the lake delineation accuracy (cf. Fujita et al. 2009; Wang et al. 2012) and the lake extent determined. Smaller lakes delineated from medium-resolution images (e.g. Landsat-7 ETM+ 30 m

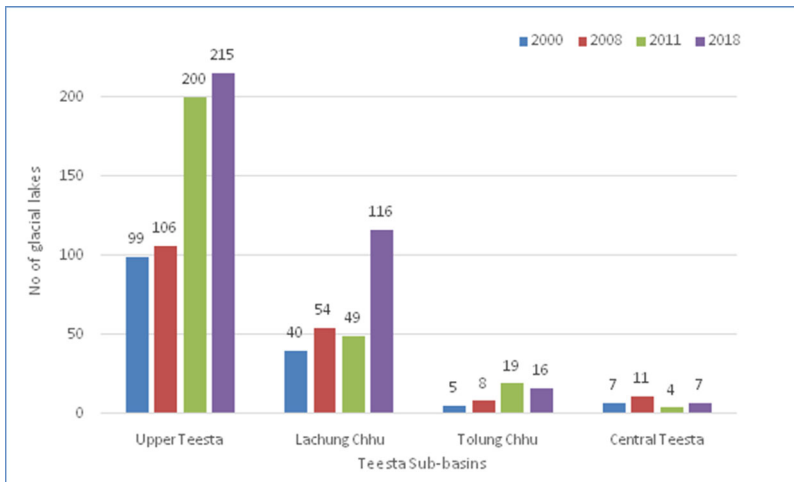


Figure 6. Number of glacial lakes in the different sub-basins of the Teesta in North Sikkim.

resolution images for the year 2000 dataset) reported the highest mean uncertainty percentage. Within the same year's inventory, mean uncertainty decreased markedly for lakes of higher size classes, with this range being the greatest within the Landsat-7 ETM+ dataset. However even within this coarser dataset, the mean uncertainty levels for the larger lakes ($> 0.5 \text{ km}^2$) was less than 10%. These results were quite similar to those derived by Debnath et al. (2018), Shukla et al. (2018) and Begam and Sen (2019) for the same region. In the other medium-resolution dataset obtained from ResourceSat-1 LISS-III images (23.5 m resolution) for 2008, the mean uncertainty percentage decreased for every lake size class as compared to the year 2000 dataset, with this value for the larger lakes being 7.68%. Derived from the highest resolution images (LISS-IV MX 5.8 m resolution), the inventories of 2011 and 2018 reported the lowest mean uncertainty values. These were extremely low for the larger lakes delineated (i.e. mean values of 4.72% and 2.29%, respectively, for lakes larger than 0.5 km^2 in the 2011 and 2018 datasets), with this yielding better results than most previous studies conducted in this region. This enhanced accuracy level was possibly achieved due to the high-resolution images used and since the lake delineation was done manually and was not dependent on direct extraction via band combination or ratioing (viz. from NDSI or NDWI indices only). Since only the medium and larger size lakes in a region pose a significant GLOF threat (Nie et al. 2017), the very low mean uncertainty values obtained for the 2018 dataset provided the validation required to subsequently use this dataset for GLOF susceptibility estimation with far greater accuracy, than was possible in most prior studies in this region. Furthermore, as the equations used by Huggel et al. (2002) to estimate each lake's depth and volume are a direct function of the lake area parameter, the computed uncertainty values for the area parameter can be feasibly taken to be indicative of the same for these variables too. However, these equations are construed based on studies conducted on European lakes, and equations that are more specifically framed, based on analysis of Himalayan lakes, would possibly reduce the uncertainty even further.

5.3. Assessing the GLOF susceptibility

The likely GLOF susceptibility of all 354 lakes in the 2018 repository was ascertained using the criteria listed in Section 4.5 (Figure 7). The salient findings were:



Table 4. Inventory of glacial lakes based on lake area in North Sikkim.

Lake area (m ²)	2000			2008			2011			2018		
	No	Total area (km ²)	Average area (km ²)	No	Total area (km ²)	Average area (km ²)	No	Total area (km ²)	Average area (km ²)	No	Total area (km ²)	Average area (km ²)
<10,000	6	0.05	0.01	21	0.13	0.01	107	0.46	0.004	138	0.69	0.005
10,000–50,000	69	1.96	0.03	76	2.07	0.03	96	2.20	0.023	130	3.23	0.025
50,000–100,000	31	2.36	0.08	35	2.61	0.07	27	1.98	0.073	31	2.30	0.074
100,000–500,000	36	6.44	0.18	37	6.65	0.18	33	6.27	0.190	44	8.51	0.193
>500,000	9	7.58	0.84	10	8.23	0.86	9	8.84	0.982	11	10.60	0.963
Total	151	18.39		179	19.69		272	19.76		354	25.33	

Source: Prepared by the authors on basis of analysis of satellite images.

Table 5. Inventory of glacial lakes based on lake depth in North Sikkim.

Lake depth (m)	2000			2008			2011			2018		
	No	Total area (km ²)	Average depth (m)	No	Total area (km ²)	Average depth (m)	No	Total area (km ²)	Average depth (m)	No	Total area (km ²)	Average depth (m)
>30	4	4.58	1.15	5	5.33	1.07	7	7.68	1.10	6	7.51	1.25
30–20	10	4.86	0.49	10	4.60	0.46	7	2.96	0.43	14	6.15	0.44
20–10	60	6.83	0.11	65	7.44	0.11	53	6.35	0.12	64	7.64	0.12
10–5	71	2.07	0.03	78	2.17	0.03	98	2.31	0.02	130	3.32	0.03
<5	6	0.05	0.01	21	0.13	0.01	107	0.46	0.07	140	0.71	0.01
Total	151	18.39		179	19.69		272	19.76		354	25.33	

Source: Prepared by the authors on basis of analysis of satellite images.

Table 6. Inventory of glacial lakes based on lake volume in North Sikkim.

Lake volume (m ³)	2000				2008				2011				2018							
	Total area (km ²)		Total volume (m ³)		Average volume (m ³)		Total area (km ²)		Total volume (m ³)		Average volume (m ³)		Total area (km ²)		Total volume (m ³)		Average volume (m ³)			
	No	(km ²)	Volume (m ³)	Average volume (m ³)	No	(km ²)	Volume (m ³)	Average volume (m ³)	No	(km ²)	Volume (m ³)	Average volume (m ³)	No	(km ²)	Volume (m ³)	Average volume (m ³)	No	(km ²)	Volume (m ³)	Average volume (m ³)
>10,000,000	10	8.06	264,829,283	26,482,928.26	10	8.23	269,572,701	26,957,270.05	10	9.29	322,692,067	32,269,206.71	12	11.04	385,308,349	32,109,029.06				
10,000,000–1,000,000	45	6.88	114,713,157	2,549,181.26	49	7.73	130,706,564	2,667,480.90	42	6.73	114,333,131	2,722,217.42	56	9.22	159,608,650	2,850,154.46				
1,000,000–500,000	21	1.43	16,087,582	766,075.31	22	1.48	16,434,861	747,039.16	16	1.02	11,177,280	698,580.00	18	1.14	12,446,949	691,497.19				
500,000–100,000	58	1.82	14,966,470	258,042.59	62	1.93	15,915,077	256,694.78	61	1.81	14,633,623	239,895.45	92	2.75	22,373,488	243,190.09				
< 100,000	17	0.19	1,029,267	60,545.14	36	0.33	1,656,864	46,024.00	143	0.91	4,244,262	29,680.15	176	1.17	5,429,971	30,852.11				
Total	151	18.39	411,625,758		179	19.69	434,286,066		272	19.76	467,080,363		354	25.33	585,167,407					

Source: Prepared by the authors on basis of analysis of satellite images.

Table 7. Lake area-wise percentage uncertainty for the four extracted inventories.

Lake area (km ²)	2000				2008				2011				2018											
	Lake Nos.		Max		Min		Mean		Lake Nos.		Max		Min		Mean		Lake Nos.		Max		Min		Mean	
	Lake Nos.	Max	Min	Mean	Lake Nos.	Max	Min	Mean	Lake Nos.	Max	Min	Mean	Lake Nos.	Max	Min	Mean	Lake Nos.	Max	Min	Mean				
< 0.01	6	98.60	60.67	77.43	21	91.25	51.02	66.98	96	70.39	14.80	31.60	138	64.19	15.26	27.24								
0.01–0.05	69	81.54	31.27	47.53	76	65.95	21.33	37.73	91	22.34	7.28	13.16	130	19.12	7.20	12.30								
0.05–0.10	31	38.46	19.94	29.01	35	37.24	15.38	22.85	26	9.56	4.85	6.91	31	10.27	5.01	7.08								
0.1–0.50	36	30.24	8.25	20.03	37	22.08	8.55	14.72	42	47.03	2.85	11.68	44	7.93	2.66	4.66								
0.5–1.0	6	15.21	9.52	11.75	6	9.66	8.14	8.83	10	19.27	1.65	8.51	6	3.36	2.31	2.65								
1.0–1.5	2	8.61	7.65	8.13	4	7.92	5.82	6.53	4	7.62	1.74	3.28	4	2.53	1.72	1.98								
1.5–2.0	1	9.99	9.99	9.99					2	5.26	2.28	3.77	1	2.24	2.24	2.24								
>2.0									1	3.32	3.32	3.32												

Source: Computed by the authors.

- i. Lake size: The maximum and minimum lake sizes were 1.76 km^2 and 524.1 m^2 , respectively [median value – $16,396 \text{ m}^2$ (approximately 0.02 km^2)]. Following Aggarwal et al. (2016), who had initially used a threshold value of 0.1 km^2 for identifying lakes prone to GLOF hazard in the same study area and had then re-denoted lakes larger than 0.6 km^2 as being the most vulnerable, we chose an overall threshold value of 0.15 km^2 to filter out the smaller lakes. Applying this to our 2018 dataset, we obtained 36 lakes which could potentially generate GLOF events. Only these 36 lakes were considered in the subsequent analysis with respect to the other parameters. The mean area of these 36 lakes was 0.47 km^2 and their mean uncertainty percentage was 3.54%.
- ii. Lake area expansion since 2011: Almost all the lakes extracted based on the above-mentioned area threshold (25 out of 36 lakes) had expanded in size from 2011 to 2018 [e.g. the Lhonak Lake (EHS_UT_085) had increased by 0.205 km^2 (Figure 7(a))], with the mean expansion value of all lakes being 0.10 km^2 . The greatest expansion recorded was 0.43 km^2 for Lake EHS_LC_020. This lake in the Lachung Chhu sub-basin had consequently experienced the maximum change amount of 97.32%. Slower growth rates (15.5% and 4.3%, respectively) were recorded for the

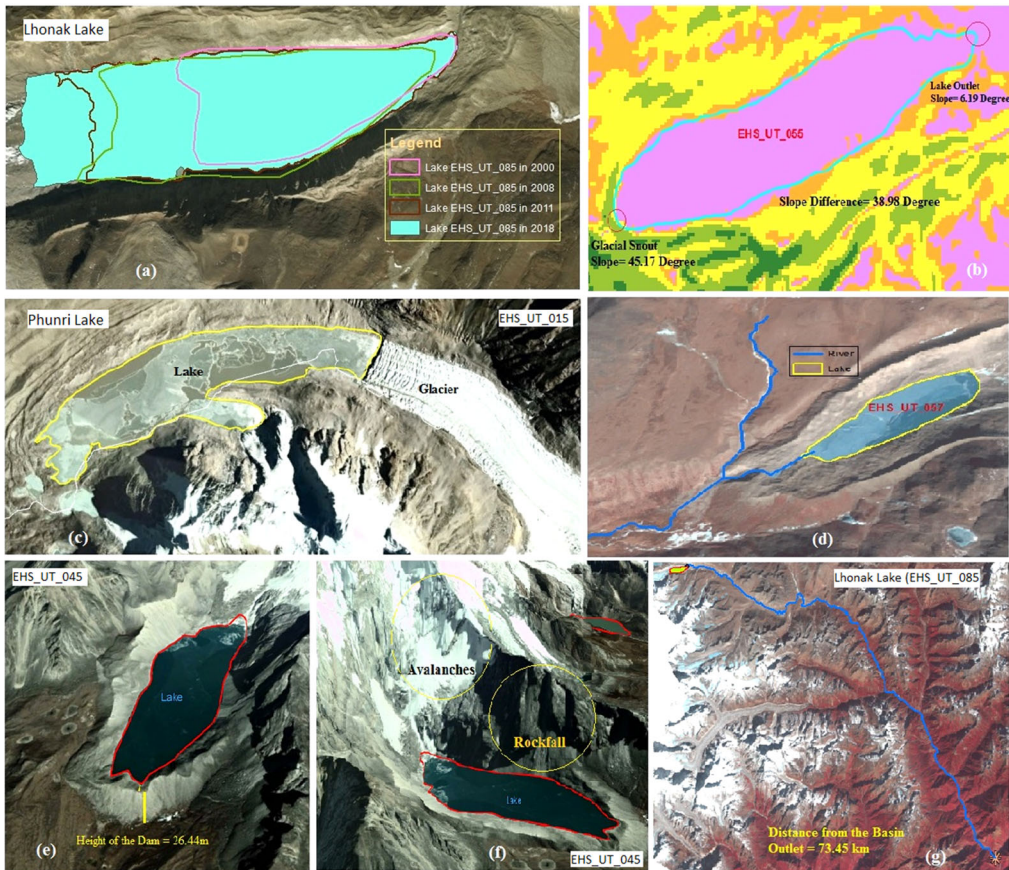


Figure 7. Examples of the multiple criteria used to categorize the GLOF hazard susceptibility for individual lakes, showing (a) lake area changes over time, (b) slope difference between glacier snout and lake outlet, (c) connection of the lake with parent glacier, (d) connection of the lake with a river, (e) height of the dam at the lake outlet, (f) availability of rocks or debris for rockfall along the lake periphery, and (g) the lake distance from the basin outlet.

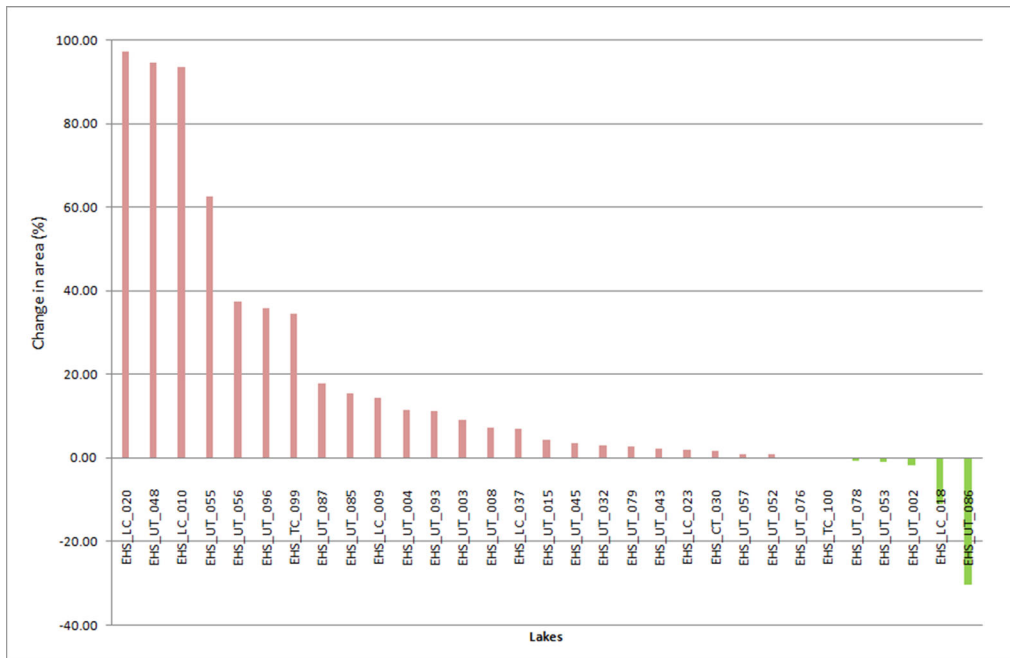


Figure 8. Changes in the lake area of GLOF hazard prone lakes in North Sikkim (2011–2018).

more commonly studied Lhonak (EHS_UT_085) and Phunri (EHS_UT_015) lakes, during the observation period (Figure 8). Five of the 36 lakes were not present in the 2011 dataset and so this parameter was not ascertained for them. However, this finding is significant as it seemingly points to newer lakes forming in this region, which can later become susceptible to GLOF events. A negative change in the lake area was recorded for six lakes, with lakes EHS_UT_086 and EHS_LC_018 shrinking by 0.17 km^2 (30.4%) and 0.03 km^2 (11.1%), respectively. This may have occurred from part in-filling of the lake with moraine deposits, rockfalls or seepage (or even due to an undetected GLOF event that emptied it partially) and needs further investigation. Rapid or marked lake shrinkage could also have connotations for future GLOF events, in terms of reducing the lake area and thus its storage capacity, thereby facilitating meltwater overspill during thaws.

- iii. Slope difference from glacier snout to lake outlet: Obviously, the slope values at the glacial snouts (maximum: 46.4° ; mean: 19.4°) were higher than those at lake outlets (maximum: 34.4° ; mean: 7.4°). Most of the lakes in the Upper Teesta sub-basin were located at higher elevations and had marked slope differences between their adjacent glacier snout and their own outlet. The highest such value (39°) was recorded for the Lake EHS_UT_055 (Figure 7(b)), while the mean for all 36 lakes was 12° .
- iv. Connection between parent glacier and river channel: Twelve of the 36 lakes were attached with a mother glacier while 17 others were located at a mean distance of 1.5 km from one (maximum: 3.9 km; minimum: 142 m). About 22 of the 36 lakes had a stream outlet, indicating their ready ability to generate a GLOF event, while 12 others were located at a mean distance of 2.7 km from a channel (maximum: 4.7 km; minimum: 598 m). Nine lakes were connected to both a glacier as well as a stream (e.g. EHS_UT_015 and EHS_UT_057 in Figure 7(c,d), respectively) and these

- posed the greatest threat of a GLOF event as the ready supply of glacial meltwater along with an available outlet could enable rapid and high discharge from such lakes.
- v. Rockfall and avalanche possibilities: Lake EHS_UT_045 was one of the many lakes in this area that was exposed to such a scenario (Figure 7(f)), with a steep scarp adjacent to the lake. In all, 22 of the 36 lakes reported similar conditions.
 - vi. Distance from the basin outlet point: Lakes were located on average 61.6 km away from their basin outlet (maximum: 91.7 km; minimum: 19.1 km). In respect of solely this parameter, lakes like the Lhonak (Figure 7(g)) were likely to pose a lower GLOF threat as it was located quite far (73.5 km) from the basin outlet.
 - vii. Height of the lake outlet dam: All the 36 lakes had adjacent moraine dams. These ranged in height from 66.4 to 5.1 m (mean: 21.6 m). For example, the Lake EHS_UT_045 had a 26.4 m high dam at its outlet (Figure 7(e)), the breaching of which could create a GLOF event.

The weights assigned on the basis of the above parameters for each lake (as per Table 2) were summed to obtain the respective CWs (see Supplementary Information Table S7). Based on this CW value, the most vulnerable or susceptible lakes were identified (Table 8, Figure 9) and accorded a corresponding hazard status (High, Medium or Low). Of the 36 lakes, 10 were categorized as being highly hazardous, 17 were of medium rating and the remaining nine lakes were at low susceptibility of causing a GLOF event. The Upper Teesta sub-basin had the highest number of these lakes, containing all the nine low, ten medium and seven high hazardous/susceptible lakes. The Lachung Chhu sub-basin had three high and four medium hazard lakes while the Tonlung Chhu and the Central Teesta sub-basins had only two and one medium hazard lakes, respectively. Almost all the 36 lakes were situated along the main snowline and Great Himalayan water divide that defines Sikkim's northern border in the Upper Teesta sub-basin, with the majority being present in the north-eastern part of this region. The few similarly hazardous lakes in the Lachung Chhu area were also proximate to these lakes. Thus the north-eastern sector of Sikkim is likely to form the main source region of any GLOF events that can afflict the downstream reaches of the state. The presence of medium and lower hazard category lakes in the cluster formed by the 10 most hazardous lakes (Figure 10), especially where they lie adjacent to each other or are situated upstream-downstream from each other along the same valley, further enhances the GLOF susceptibility as a snowballing effect could result, with the outflow from one lake cascading into another and causing it to breach as well. Furthermore, where these lakes are connected with a glacier (as is seen to be the case for almost all the highly hazardous lakes in their Google Earth screenshots – Figure 10), future glacial melt/retreat due to rising temperatures shall augment the lake volume and increase the chances of a GLOF event, especially where the lake is also linked with a downstream channel.

5.4. Climate data analysis

Rising temperatures facilitate greater glacial melt and enhanced formation/expansion of glacial lakes (Quincey et al. 2007; Veh et al. 2020), with this subsequently leading to GLOF events in the Himalayas (Mir et al. 2018). Therefore a detailed analysis of the principal climatic parameters in any such study is most pertinent (Benn et al. 2012; Liu et al. 2014). Previous studies have highlighted the marked climate changes occurring within the Himalayas (Chaudhary et al. 2011), commenting on the unpredictability of the region's

Table 8. Potentially hazardous lakes in terms of GLOF events.

Lake code	Area change from 2011 to 2018 (km ²)	Slope difference between glacier snout and lake outlet (in °)	Connection to glaciers (Y/N)	Connection with channel (Y/N)	Height of the Dam (m)	Availability of rocks for avalanches (Y/N)	Distance from the outlet basin (km)	Cumulative weight (CW)	Hazard ranking
EHS_UT_055	0.4	39.0	Y	Y	17.8	Y	61.5	19	High
EHS_UT_043	0.0	28.0	Y	Y	17.7	Y	58.8	18	High
EHS_UT_056	0.2	19.9	N	Y	11.4	Y	55.9	17	High
EHS_LC_023	0.0	17.6	Y	Y	25.6	Y	47.8	17	High
EHS_UT_004	0.1	17.8	Y	Y	20.5	Y	80.8	16	High
EHS_UT_085	0.2	7.8	Y	Y	17.6	Y	73.5	16	High
EHS_UT_048	0.3	17.9	Y	N	18.0	N	69.2	16	High
EHS_LC_010	0.3	9.0	N	Y	14.8	Y	53.2	16	High
EHS_LC_020	0.4	18.1	N	N	19.9	Y	52.2	16	High
EHS_UT_045	0.0	28.8	Y	N	26.4	Y	56.3	16	High

Source: Prepared by the authors.

Note: The details of only the most hazardous category of glacial lakes identified in the study area have been shown in Table 9. For hazard status of all 36 lakes evaluated, see Supplementary Table S7.

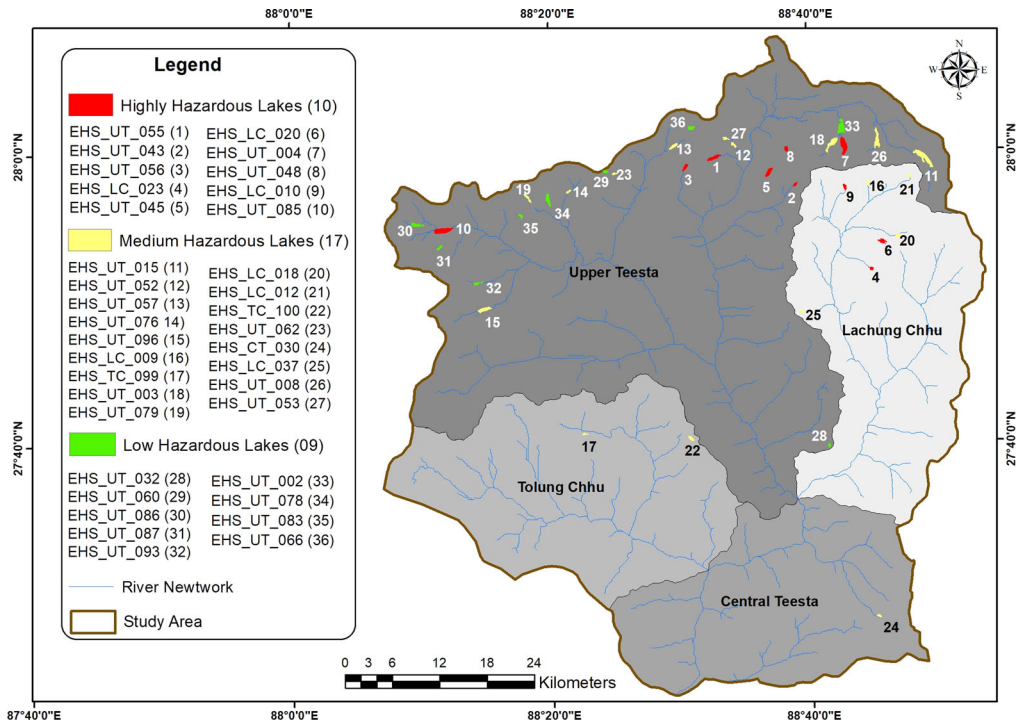


Figure 9. Potentially dangerous lakes susceptible to GLOF events in North Sikkim.

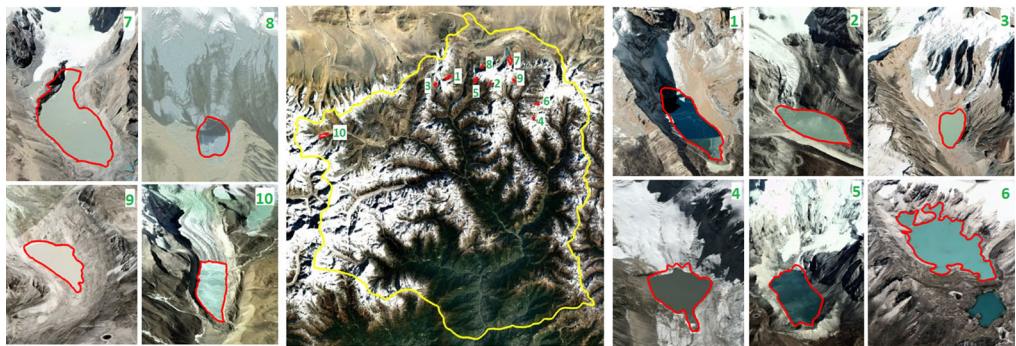


Figure 10. Google Earth screenshots of the ten most hazardous lakes in terms of GLOF events in the Sikkim Himalayas (Note: The numerical labels given to each lake within the figure correspond to their notations as denoted in Figure 9).

weather and rapid rates of snowmelt (Sharma et al. 2009; Chaudhary and Bawa 2011). Two sets of temperature and precipitation data were analyzed separately. The first was the long-term data (1901–2002) obtained from the India Water Portal, specifically for North Sikkim district. The second was the more recent shorter term gridded dataset obtained from IMD, which though centering on North Sikkim, covered a slightly larger area. Due to their slightly differing geographies, we did not combine them together but performed the same analysis separately (Figure 11). From the long-term dataset, a discernable mean annual temperature rise of about 0.5 °C over the 102 years’ time period was noted (Figure 11(a)). From the shorter term gridded dataset (1990–2015) covering a larger areal extent, this rise was higher, about 1.5 °C (Figure 11(c)), possibly since it included the southern

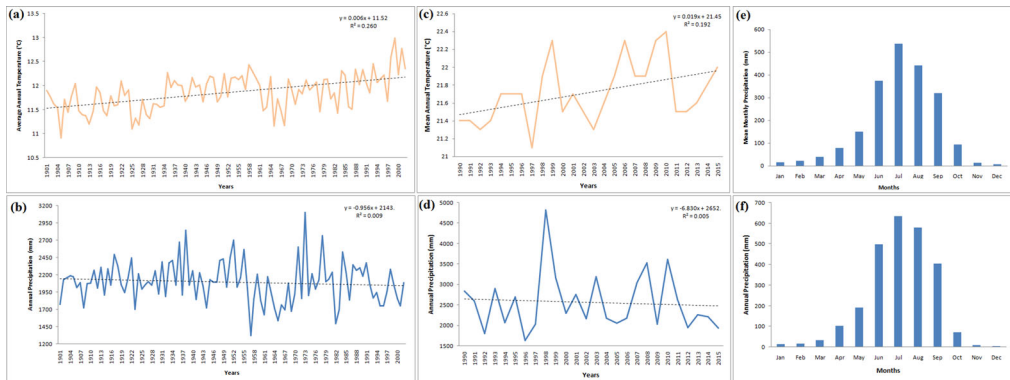


Figure 11. Changes and trends in climate parameters in the study area – (a) and (b) show long-term mean annual temperature and annual precipitation trends (1901–2002) specifically for North Sikkim district, (c) and (d) show more recent and shorter term (1990–2015) mean annual temperature and annual precipitation trends for the Sikkim region, (e) and (f) are the mean monthly precipitation as derived from the two datasets (1901–2002 and 1990–2015), respectively.

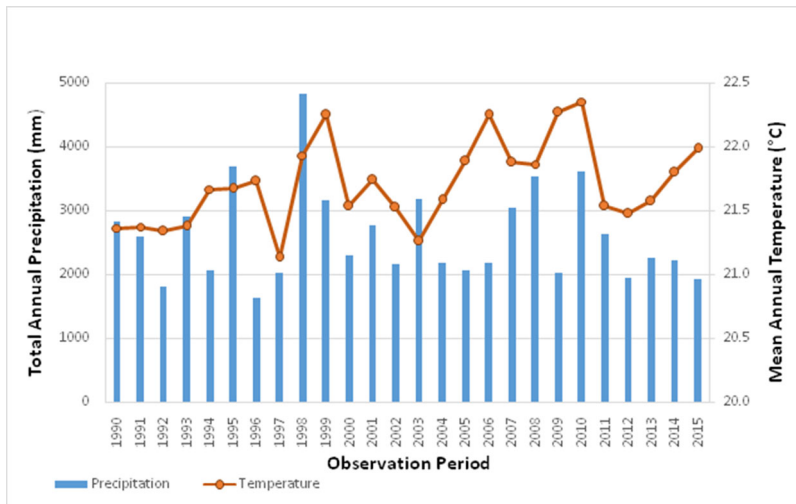


Figure 12. Average annual temperature and precipitation regime in Sikkim (derived from the gridded climate data for Sikkim from 1990 to 2015 – tile centroid at 27°50'00"N and 88°50'00"E in North Sikkim district).

parts of Sikkim too. However the R^2 values of the respective trends are quite low (0.260 for the long-term IMD dataset and 0.192 for the shorter term gridded dataset), due to the data variability. Mean temperature trends of just the spring and summer monsoon months (for both datasets) showed a discernable increase in each case ([Appendix A – Figures A.1 and A.2](#)), with the gridded dataset exhibiting a more pronounced rise. Particularly, the marked rise in the mean temperature of March is significant (about 1 °C during 1901–2002 and 1.5 °C during 1990–2015), and to a lesser extent that of April and May, which likely indicates greater spring and summer thaws. This shall augment lake volumes further and thereby reduce lake capacities for holding the subsequent monsoonal deluge, thus increasing the chances of a GLOF event.

The above results are further substantiated by the outputs of the performed Mann-Kendall test on both the long-term (1901–2002) and short-term (1990–2015) temperature

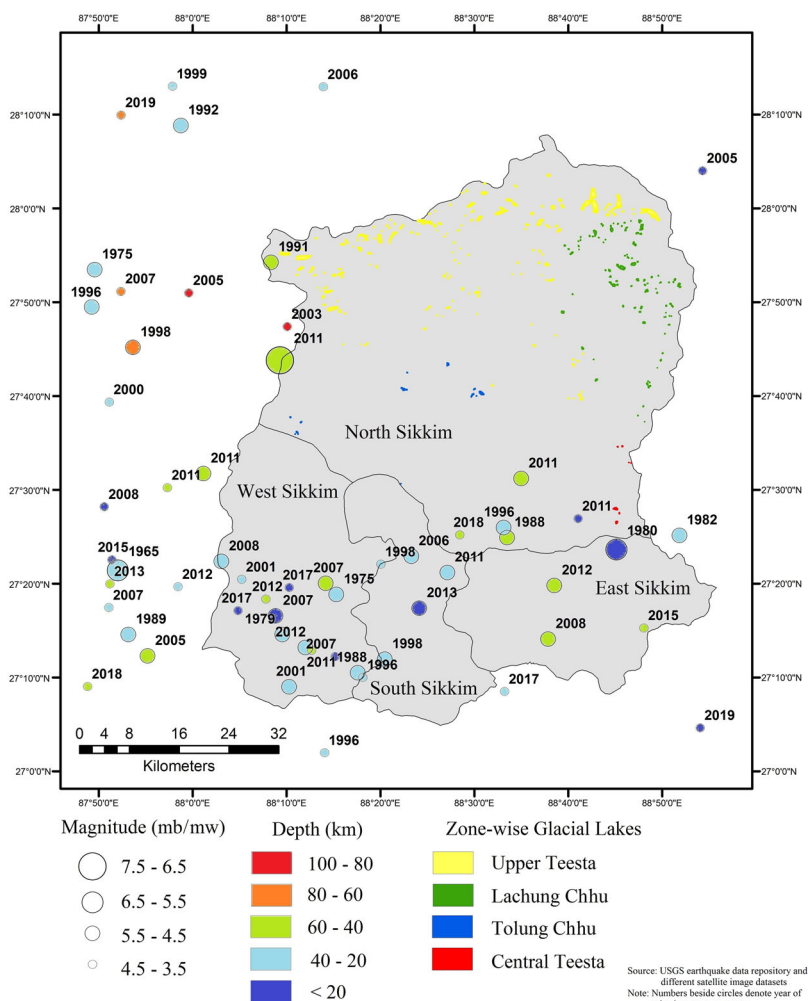


Figure 13. Recent seismicity map of Sikkim and its adjacent areas.

datasets (see [Tables A.1](#) and [A.2](#) in [Appendix A](#)). We elicited the trends for the average annual temperature, the mean temperature of the warmest months in a year (March–June) and the mean temperature of the coldest months of each year (January, February, November and December). For the long-term dataset, in each of the above three cases, the derived p -value was lower than the significance level α value of 0.05, indicating the presence of a trend in the dataset. The positive MK test Statistic (S) values and the positive Sen’s slope values further indicated an upward trend ([Karmeshu 2012](#)), signifying that the mean temperature values had indeed increased over time. The same was observed for the annual average temperature of the short-term dataset, which also showed an increasing trend over time. However, the average temperatures of the warmest or coldest months in this dataset did not show any discernable trend.

Annual precipitation trends (for both datasets) show a slight decline ([Figure 11\(b,d\)](#)), while its seasonality seems to have become more pronounced ([Figure 11\(e,f\)](#)), i.e. more rainfall during the monsoon months. Monthly variations of mean temperature and rainfall at five year intervals during 1990–2015 ([Appendix A –Figure A.3](#)) as discerned from the

gridded dataset confirms the predominantly summer monsoonal climatic regime of Sikkim (cf. Basnett et al. 2013). The mean annual temperature ranges from 21.1 °C to 22.4 °C while the annual precipitation ranges between 1632.9 to 4820.3 mm over this 26 year observation period. These results are similar to those obtained by Tambe et al. (2011) and Debnath et al. (2019) for the same region. Particularly from 2011 onwards, a steady increase in the mean annual temperature and decrease in the total yearly precipitation is apparent (Figure 12). These may be potential reasons for the increase in glacial lakes from 272 to 354 between 2011 and 2018, due to enhanced melting and lowered replenishment of the glacial mass (which exposes the underlying surface, thereby allowing it to absorb more heat and facilitate further melt).

5.5. Discussion

The distribution, shape, orientation and dimensions of the lakes demarcated in this study matched quite well with those documented in the glacial lakes database (only the more significant and larger lakes are part of this repository) prepared under the National Hydrology Project by the Ministry of Jal Shakti, Government of India (see <http://indiaw-ris.gov.in/wris/#/about>). Furthermore, the very low mean uncertainty percentage in the computed lake dimensions compared favourably with similar studies in the same region (e.g. Shukla et al. 2018; Begam and Sen 2019). This dual validation allowed us to undertake the further components of the study. We have also importantly documented lakes that have traditionally not been regarded as GLOF hazards and thus found scant mention in the literature (cf. Raj et al. 2013a, 2013b; Begam et al. 2018), underlining the importance of conducting such inventory studies on a regular basis for repeatedly recording the status of known/newer lakes in this region. This is also one of the few studies that has utilized high-resolution images for glacial lake mapping in Sikkim (besides Aggarwal et al. 2017), thus overcoming some of the inherent constraints of using medium resolution images (Landsat/LISS-III) for this purpose (e.g. Raj et al. 2013b; Debnath et al. 2018; Shukla et al. 2018). However, the use of a higher resolution DEM would have elicited a more accurate terrain dataset (Das et al. 2016) and enhanced the resultant analysis. Our accorded ratings of High, Medium and Low Hazard status for the different lakes matches on a number of points with the ratings given by Aggarwal et al. (2017) to the same lakes (e.g. the Lhonak Lake (EHS_UT_085) and the EHS_UT-004 lake have been demarcated as being most hazardous in both studies). There are several other matches in the medium- and low-hazard lake category, while our rating system has also accorded a slightly higher susceptibility category to some lakes than that accorded by Aggarwal et al. (2017). However, as outlined in the same paper, the AHP-based weightage method used by Aggarwal et al. (2017) can also induce bias and thus our scheme of weighing all factors on a uniform scale seems more prudent.

Glacier extent losses around 3.3% have occurred between 1990 and 2010 in the Sikkim Himalayas, mainly due to rising temperatures (Basnett et al. 2013), transforming debris-covered supraglacial lakes into large moraine-dam lakes. We show a 2% increase in the mean annual temperature just between 2011 and 2015, which is considered to be most favourable for glacier retreat in the Himalayas (Singh and Kumar 1997; Singh et al. 2006; Xu et al. 2016; Kraaijenbrink et al. 2017). This could have spurred on the formation of 82 new lakes in North Sikkim since 2011. Rising lake temperatures in Sikkim (Debnath et al. 2018) has also induced glacier retreat, with this considered to be a significant factor behind the tremendous increase in the area of the Lhonak Lake (EHS_UT_085) during 1976 to 2007 (Kulkarni et al. 2011). This region received a high average annual

precipitation of 2560 mm during the observation period (1990–2015), 82% of which occurred during June to September (cf. Bertolani et al. (2000) in the Everest Himalayas). Such concentrated rainfall spells often induce mass movements, which is one of the biggest triggers of GLOF events in the Indian, Nepal and Bhutan Himalayas (Prakash and Nagarajan 2017; Rounce et al. 2017; Allen et al. 2019). They also generate flash floods, mudflows and landslides in the lower reaches of the Teesta Basin (Mandal and Chakrabarty 2016; Pal et al. 2016). Such events therefore pose a constant threat to the downstream infrastructure and vulnerable communities who reside along this region's valleys (Basu 2015). Mitigation plans have therefore been framed by the Government of Sikkim to siphon off excess lake water from rapidly expanding sites like the Lhonak Lake while at the same time organizing awareness programmes to increase community resilience and prepare evacuation plans (Shrestha 2018; SSDMA 2019).

Some studies have considered the impact of seismicity on GLOF events (e.g. Gurung et al. 2017; Prakash and Nagarajan 2017; Cook et al. 2018) as these can induce moraine dam breaches through piping (Richardson and Reynolds 2000) as well as engender mass movements into glacial lakes. We did not actively consider this parameter in the weight-age scheme for reasons outlined in section 4.5. The entire state of Sikkim falls under Zone IV (High Damage Risk Zone) as per the Seismic Hazard Zonation of India (BTMPC, 2019). While North Sikkim district does have a few recent earthquake epicentres (from 1965 to 2019 – Figure 13), these are far higher in both number and magnitude in West Sikkim district and further to the west (as per the USGS database). A 6.9 magnitude earthquake in 2011 within/adjacent to the western border of North Sikkim was the highest recorded in this district, whose epicentre lay close to some of the glacial lakes in the Upper Teesta sub-basin. Another 6.1 magnitude seismic event in East Sikkim district in 1980, close to the location of the Central Teesta sub-basin glacial lakes, was the next highest occurrence. During the recent 2015 Gorkha Earthquake, a number of GLOF events were reported from the surrounding regions of Nepal (MoHA and DPNNet, 2015; Byers et al. 2017; Cook et al. 2018; Sunuwar 2018; Liu et al. 2020). However, this earthquake does not seem to have triggered GLOF events in the Sikkim Himalayas and we did not find any studies documenting the same. However, as stated previously, seismic events (and repeat earthquakes) have the potential to trigger GLOF events in faraway locations and with alpine glacial lakes obviously forming mostly within active high mountain tectonic belts (Emmer and Cochachin 2013), this remains a possibility in North Sikkim.

6. Conclusion

This study has generated a high-resolution recent inventory of glacial lakes in a part of the Sikkim Himalayas, to augment similar databases created previously for this region. Lakes were delineated manually and cross-checked for validation with Google Earth images. The GLOF susceptibility for these lakes was also assessed, based on a range of parameters defined in the literature. Through this, 36 lakes were identified as hazardous, of which, 10 were noted to be highly susceptible. In this respect, the Upper Teesta and Lachung Chhu sub-basins were ascertained as the most likely source regions of any GLOF events that may occur here. However, we propose that the other 26 lakes that were classified as being of medium and low hazard status, be also monitored and re-evaluated regularly, since changes in their parameters can elevate them into more enhanced hazard categories. Furthermore, the study also revealed the recent trends in this area's mean annual temperature and annual precipitation, as recorded during a 26 year observation period (1990–2015). These could be influencing factors behind the noted sharp increase in the number of new glacial lakes

formed between 2011 and 2018, possibly due to a regional climatic variability induced glacial retreat/melting. However, further in-depth research is required to better ascertain such relationships. We also showed that the overall lake area in North Sikkim had increased by 6.9 km² during the study period of 2000–2018 (a rise of 37.5%). Regular monitoring of the environmental conditions of the glacial lakes in this region through the integration of remotely sensed high-resolution data with field investigations is therefore sorely required for continuously evaluating the GLOF threat along with the establishment of Early Warning Systems that can convey the ambient threat quickly to the downstream communities. While some such facilities have been installed (e.g. at Shakho Chho Glacial Lake in North Sikkim – C-DAC 2018), more such endeavours are required to safeguard the local settlements and infrastructure against such GLOF hazards.

Acknowledgement

The authors are grateful to the teaching and non-teaching (field-store) staff of the School of Geography, University of Leeds, UK for their continuous support in developing the ideas for this work and guidance during its various phases. The authors most gratefully acknowledge Dr. Duncan J. Quincey of the School of Geography, University of Leeds, United Kingdom (MSc Dissertation guide of Nazimul Islam), for his valuable comments on the work from time to time. The authors are also most grateful to the Priestley International Centre for Climate (PICC) for the financial support given for this study. The very detailed suggestions received from multiple reviewers and the ADM, Prof. Bradley Rundquist, helped to improve the manuscript immeasurably and to them we express our sincere thanks.

Disclosure statement

The authors report no potential conflict of interest.

Funding

This study was funded by the Climate Bursary Award of Priestley International Centre for Climate Change (PICC), University of Leeds, United Kingdom, awarded to Nazimul Islam for purchasing satellite images, meteorological data and to conduct a short fieldwork in the Upper Teesta Basin of Sikkim Himalaya.

ORCID

Nazimul Islam  <http://orcid.org/0000-0002-5295-3773>

Priyank Pravin Patel  <http://orcid.org/0000-0003-4990-1662>

Data availability statement

The authors confirm that most of the data supporting the findings of this study are available within the article, in the links provided [and/or] in its [supplementary materials](#).

References

- Aggarwal A, Jain SK, Lohani AK, Jain N. 2016. Glacial lake outburst flood risk assessment using combined approaches of remote sensing, GIS and dam break modelling. *Geomatics Nat Hazards Risk*. 7(1): 18–36.
- Aggarwal S, Rai SC, Thakur PK, Emmer A. 2017. Inventory and recently increasing GLOF susceptibility of glacial lakes in Sikkim. Eastern Himalaya. *Geomorphology* 295:39–54.

- Allen SK, Frey H, Huggel C. 2017. Assessment of glacier and permafrost hazard in mountain regions – technical guide document. Standing group on glacier and permafrost hazards in mountains (GAPHAZ) of the International Association of Cryospheric Sciences (IACS) and the International Permafrost Association (IPA). Zurich, Switzerland/Lima, Peru: Sponsored by Swiss Agency for Development and Cooperation (SDC).
- Allen SK, Zhang G, Wang W, Yao T, Bolch T. 2019. Potentially dangerous glacial lakes across the Tibetan Plateau revealed using a large-scale automated assessment approach. *Science Bull.* 64(7): 435–445.
- Anderson JR, Hardy EE, Roach JT. 1976. A land use and land cover classification system for use with remote sensor data. Alexandria, VA: US Geological Survey; [accessed 2018 Aug 26]. <https://pubs.usgs.gov/pp/0964/report.pdf>
- Bajracharya SR, Mool PK, Shrestha BR. 2007. Impact of climate change on Himalayan glaciers and glacial lakes: Case studies on GLOF and associated hazards in Nepal and Bhutan. Kathmandu (Nepal): ICIMOD and UNEP/ROAP; [accessed 2018 Dec 20]. http://lib.icimod.org/record/22442/files/attachment_169.pdf
- Basnett S, Kulkarni AV, Bolch T. 2013. The influence of debris cover and glacial lakes on the recession of glaciers in Sikkim Himalaya. *J Glaciol.* 59(218):1035–1046.
- Basu S. 2015 Aug 17. Sikkim at risk of devastating floods from glacial lake outbursts. *DownToEarth*; [accessed 2019 May 15]. <https://www.downtoearth.org.in/news/sikkim-at-risk-of-devastating-floods-from-glacial-lake-outbursts--40313>
- Begam S, Sen D. 2019. Mapping of moraine dammed glacial lakes and assessment of their areal changes in the central and eastern Himalayas using satellite data. *J Mt Sci.* 16(1):77–94.
- Begam S, Sen D, Dey S. 2018. Moraine dam breach and glacial lake outburst flood generation by physical and numerical models. *J Hydrol.* 563:694–710.
- Benn DI, Bolch T, Hands K, Gulley J, Luckman A, Nicholson LI, Quincey D, Thompson S, Toumi R, Wiseman S. 2012. Response of debris-covered glaciers in the Mount Everest region to recent warming, and implications for outburst flood hazards. *Earth Sci Rev.* 114(1–2):156–174.
- Bertolani L, Bollasina M, Tartari G. 2000. Recent biennial variability of meteorological features in the Eastern Highland Himalayas. *Geophys Res Lett.* 27(15):2185–2188.
- Bohner J, Lehmkühl F. 2005. Environmental change modelling for central and high Asia: Pleistocene, present and future scenarios. *Boreas.* 34(2):220–231.
- Bolch T, Kulkarni A, Kaab A, Huggel C, Paul F, Cogley JG, Frey H, Kargel JS, Fujita K, Scheel M, et al. 2012. The state and fate of Himalayan Glaciers. *Science.* 336(6079):310–314.
- Bolch T, Peters J, Yegorov A, Pradhan B, Buchroithner M, Blagoveshchensky V. 2011. Identification of potentially dangerous glacial lakes in the northern Tien Shan. *Nat Hazards.* 59(3):1691–1714.
- BTMPC (Building Materials & Technology Promotion Council). 2019. Ministry of Housing & Urban Affairs, Government of India. New Delhi (India). Vulnerability Atlas of India (Third Edition); [accessed 2020 Apr 24]. <http://bmtpc.org/DataFiles/CMS/file/VAI2019/Index.html>
- Byers AC, III, Byers EA, McKinney DC, Rounce DR. 2017. A field-based study of impacts of the 2015 earthquake on potentially dangerous glacial lakes in Nepal. *Himalaya.* 37(2):26–41.
- Campbell JG. 2005. Inventory of glaciers, glacial lakes and the identification of potential glacial lake outburst floods (GLOFs) affected by Global Warming in the mountains of India, Pakistan and China/Tibet autonomous region. Kathmandu (Nepal): ICIMOD and Asia Pacific Network (APN) technical report; [accessed 2018 Aug 26]. <https://www.apn-gcr.org/resources/files/original/d71dea72b-c764245642e7d047c095463.pdf>
- C-DAC (Centre for Development of Advanced Computing) 2018. Glacier lake management & GLOF early warning system. New Delhi (India): Ministry of Electronics and Information Technology (MeitY), Government of India; [accessed 2020 Apr 24]. https://www.cdac.in/index.aspx?id=st_ssdm_ssdm_glof
- Chand P, Sharma MC. 2015. Glacier changes in the Ravi basin, North-Western Himalaya (India) during the last four decades (1971–2010/13). *Glob Planet Change.* 135:133–147.
- Chaudhary P, Bawa KS. 2011. Local perceptions of climate change validated by scientific evidence in the Himalayas. *Biol Lett.* 7(5):767–770.
- Chaudhary P, Rai S, Wangdi S, Mao A, Rehman N, Chettri S, Bawa KS. 2011. Consistency of local perceptions of climate change in the Kangchenjunga Himalaya landscape. *Curr Sci.* 101(4):504–513.
- Clague JJ, O'Connor JE. 2015. Glacier-related outburst floods. In: Haeblerli W, Whiteman C, editors. *Snow and ice-related hazards, risks, and disasters*. Amsterdam: Elsevier; p. 487–519.
- Cook KL, Andermann C, Gimbert F, Adhikari BR, Hovius N. 2018. Glacial lake outburst floods as drivers of fluvial erosion in the Himalaya. *Science.* 362(6410):53–57.

- Das S, Patel PP, Sengupta S. 2016. Evaluation of different digital elevation models for analyzing drainage morphometric parameters in a mountainous terrain: A case study of the Supin–Upper Tons Basin, Indian Himalayas. *Springer Plus*. 51:1544. <http://dx.doi.org/10.1186/s40064-016-3207-0>
- Debnath M, Sharma MC, Syiemlieh HK. 2019. Glacier dynamics in Changme Khangpu Basin, Sikkim Himalaya, India between 1975 and 2016. *Geosciences*. 9(6):259. <http://dx.doi.org/10.3390/geosciences9060259>.
- Debnath M, Syiemlieh HK, Sharma MC, Kumar R, Chowdhury A, Lal U. 2018. Glacial lake dynamics and lake surface temperature assessment along the Kangchengayo-Pauhunri Massif, Sikkim Himalaya, 1988–2014. *Remote Sens Appl Soc Environ*. 9:26–41.
- Dubey S, Goyal MK. 2020. Glacial lake outburst flood (GLOF) hazard, downstream impact, and risk over the Indian Himalayas. *Water Resour Res*. 56(4):e2019WR026533. <http://dx.doi.org/10.1029/2019WR026533>
- Emmer A, Cochachin A. 2013. The causes and mechanisms of moraine-dammed lake failures in the Cordillera Blanca, North American Cordillera, and Himalayas. *AUC Geogr*. 48(2):5–15.
- Frey H, Machguth H, Huss M, Huggel C, Bajracharya S, Bolch T, Kulkarni A, Linsbauer A, Salzmann N, Stoffel M. 2014. Estimating the volume of glaciers in the Himalayan–Karakoram region using different methods. *Cryosphere*. 8(6):2313–2333.
- Fujita K, Sakai A, Nuimura T, Yamaguchi S, Sharma RR. 2009. Recent changes in Imja Glacial Lake and its damming moraine in the Nepal Himalaya revealed by in situ surveys and multi-temporal ASTER imagery. *Environ Res Lett*. 4(4):045205. <http://dx.doi.org/10.1088/1748-9326/4/4/045205>
- Gardelle J, Arnaud Y, Berthier E. 2011. Contrasted evolution of glacial lakes along the Hindu Kush Himalaya Mountain Range between 1990 and 2009. *Glob Planet Change*. 75(1-2):47–55.
- Geological Survey of India (GSI) 2012. Geology and mineral resources of Sikkim. Kolkata: GSI, Eastern region; [accessed 2018 Aug 26]. http://www.sikennis.nic.in/WriteReadData/UserFiles/file/GSI%20Miscpub30_Sikkim.pdf
- Gilbert RO. 1987. *Statistical methods for environmental pollution monitoring*. New York: Van Nostrand Reinhold.
- Gupta V, Mahajan AK, Thakur VC. 2015. A study on landslides triggered during Sikkim Earthquake of September 18, 2011. *Himalayan Geol*. 36(1):81–90.
- Gurung DR, Khanal NR, Bajracharya SR, Tsering K, Joshi S, Tshering P, Chhetri LK, Lotey Y, Penjor T. 2017. Lemang Tsho glacial lake outburst flood (GLOF) in Bhutan: Cause and impact. *Environ Risk Assess Remediat*. 01(01):7–15.
- Hakeem KA, Abirami S, Rao VV, Diwakar PG, Dadhwal VK. 2018. Updated inventory of glacial lakes in Teesta basin using remote sensing data for use in GLOF risk assessment. *J Indian Soc Remote Sens*. 46(3):463–470.
- Hall DK, Riggs GA. 2014. Normalized-difference snow index. In: Singh VP, Singh P, Haritashya UK, editors. *Encyclopaedia of snow, ice and glaciers*. Dordrecht: Springer; p. 779–780.
- Hazra P, Krishna AP. 2019. Spatio-temporal and surface elevation change assessment of glaciers of Sikkim Himalaya (India) across different size classes using geospatial techniques. *Environ Earth Sci*. 78(14): 387.
- Huggel C, Haeberli W, Käab A, Bieri D, Richardson S. 2004. An assessment procedure for glacial hazards in the Swiss Alps. *Can Geotech J*. 41(6):1068–1083.
- Huggel C, Käab A, Haeberli W, Teyssere P, Paul F. 2002. Remote sensing based assessment of hazards from glacier lake outbursts: A case study in the Swiss Alps. *Can Geotech J*. 39(2):316–330.
- Immerzeel WW, Lutz AF, Andrade M, Bahl A, Biemans H, Bolch T, Hyde S, Brumby S, Davies BJ, Elmore AC, et al. 2020. Importance and vulnerability of the world's water towers. *Nature*. 577(7790): 364–369.
- IPCC (Intergovernmental Panel on Climate Change) 2007. Fourth assessment report – Climate change. [accessed 2018 Jul 28]. http://www.ipcc.ch/pdf/assessment-report/ar4/syr/ar4_syr_full_report.pdf
- Iribarren PA, Norton KP, Mackintosh A. 2014. Moraine-dammed lake failures in Patagonia and assessment of outburst susceptibility in the Baker Basin. *Nat Hazards Earth Syst Sci*. 14(12):3243–3259.
- Käab A, Berthier E, Nuth C, Gardelle J, Arnaud Y. 2012. Contrasting patterns of early twenty-first-century glacier mass change in the Himalayas. *Nature*. 488(7412):495–498.
- Karmeshu N. 2012. Trend detection in annual temperature & precipitation using the Mann Kendall Test – A case study to assess climate change on select states in the Northeastern United States [Master's Thesis]. Department of Earth & Environmental Science, University of Pennsylvania. [accessed 2020 Nov 20] https://repository.upenn.edu/cgi/viewcontent.cgi?article=1045&context=mes_capstones
- Kendall MG. 1975. *Rank correlation methods*. London: Charles Griffin.

- Khadka N, Zhang G, Chen W. 2019. The state of six dangerous glacial lakes in the Nepalese Himalaya. *Terr Atmos Ocean Sci.* 30(1):63–72.
- Khadka N, Zhang G, Thakuri S. 2018. Glacial lakes in the Nepal Himalaya: inventory and decadal dynamics (1977–2017). *Remote Sens.* 10:1913. <http://dx.doi.org/10.3390/rs10121913>.
- King O, Dehecq A, Quincey D, Carrivick J. 2018. Contrasting geometric and dynamic evolution of lake and land-terminating glaciers in the central Himalaya. *Global Planet Change.* 167:46–60.
- King O, Quincey DJ, Carrivick JL, Rowan AV. 2017. Spatial variability in mass loss of glaciers in the Everest region, central Himalayas, between 2000 and 2015. *Cryosphere.* 11(1):407–426.
- Kraaijenbrink PDA, Bierkens MFP, Lutz AF, Immerzeel WW. 2017. Impact of a global temperature rise of 1.5 degrees Celsius on Asia's glaciers. *Nature.* 549(7671):257–260.
- Kron W. 2005. Flood Risk = Hazard • Values • Vulnerability. *Water Int.* 30(1):58–68.
- Kulkarni AV, Rathore BP, Singh SK, Bahuguna IM. 2011. Understanding changes in the Himalayan cryosphere using remote sensing techniques. *Int J Remote Sens.* 32(3):601–615.
- Kumar A, Gupta AK, Bhambri R, Verma A, Tiwari SK, Asthana AKL. 2018. Assessment and review of hydrometeorological aspects for cloudburst and flash flood events in the third pole region (Indian Himalaya). *Polar Sci.* 18:5–20.
- Li H, Mao H, Li X, Wang Z, Wang C. 2019. Monitoring 40-year lake area changes of the Qaidam basin, Tibetan plateau, using Landsat time series. *Remote Sens.* 11(3):343. <http://dx.doi.org/10.3390/rs11030343>
- Liu J, Cheng Z, Su P. 2014. The relationship between air temperature fluctuation and glacial lake outburst floods in Tibet, China. *Quat Int.* 321:78–87.
- Liu M, Chen N, Zhang Y, Deng M. 2020. Glacial lake inventory and lake outburst flood/debris flow hazard assessment after the Gorkha earthquake in the Bhote Koshi basin. *Water.* 12(2):464. <http://dx.doi.org/10.3390/w12020464>
- Mandal SP, Chakrabarty A. 2016. Flash flood risk assessment for upper Teesta river basin: Using the hydrological modeling system (HEC-HMS) software. *Model Earth Syst Environ.* 2(2):59.
- Maskey S, Kayastha RB, Kayastha R. 2020. Glacial lakes outburst floods (GLOFs) modelling of Thulagi and lower Barun glacial lakes of Nepalese Himalaya. *Prog Disaster Sci.* 7:100106.
- McKillop RJ, Clague JJ. 2007. Statistical, remote sensing-based approach for estimating the probability of catastrophic drainage from moraine-dammed lakes in southwestern British Columbia. *Glob Planet Change.* 56(1–2):153–171.
- Mehrotra GS, Sarkar S, Kanungo DP, Mahadevaiah K. 1996. Terrain analysis and spatial assessment of landslide hazards in parts of Sikkim Himalaya. *J Geol Soc India.* 47(4):491–498.
- Mergili M, Schneider JF. 2011. Regional-scale analysis of lake outburst hazards in the southwestern Pamir, Tajikistan, based on remote sensing and GIS. *Nat Hazards Earth Syst Sci.* 11(5):1447–1462.
- Milner AM, Khamis K, Battin TJ, Brittain JE, Barrand NE, Fureder L, Cauvy-Fraunie S, Gislason GM, Jacobsen D, Hannah DM, et al. 2017. Glacier shrinkage driving global changes in downstream systems. *Proc Natl Acad Sci USA.* 114(37):9770–9778.
- Mir RA, Jain SK, Lohani AK, Saraf AK. 2018. Glacier recession and glacial lake outburst flood studies in Zaskar basin, western Himalaya. *J Hydrol.* 564:376–396.
- MoHA (Ministry of Home Affairs) and DPNet (Disaster Preparedness Network-Nepal) 2015. Government of Nepal. Kathmandu (Nepal). Nepal Disaster Report 2015. [accessed 2020 Sep 10]. <http://www.drrportal.gov.np/uploads/document/329.pdf>
- Mool PK, Wangda D, Bajracharya SR, Kunzang K, Gurung DR, Joshi SP. 2001. Inventory of glaciers, glacial lakes and glacial lake outburst floods (Monitoring and early warning systems in the Hindu Kush-Himalayan region), Bhutan. Kathmandu (Nepal): ICIMOD and UNEP/RPC-AP; [accessed 2018 Aug 26]. https://www.preventionweb.net/files/2370_InventoryGlaciers.pdf
- Nath SK, Thingbaijam KKS, Raj A. 2008. Earthquake hazard in Northeast India – A seismic microzonation approach with typical case studies from Sikkim Himalaya and Guwahati city. *J Earth Syst Sci.* 117(S2):809–831.
- Nie Y, Liu Q, Wang J, Zhang Y, Sheng Y, Liu S. 2018. An inventory of historical glacial lake outburst floods in the Himalayas based on remote sensing observations and geomorphological analysis. *Geomorphology.* 308:91–106.
- Nie Y, Sheng Y, Liu Q, Liu L, Liu S, Zhang Y, Song C. 2017. A regional-scale assessment of Himalayan glacial lake changes using satellite observations from 1990 to 2015. *Remote Sens. Environ.* 189:1–13.
- NRC (National Research Council) 2012. Himalayan glaciers: Climate change, water resources, and water security. Washington, DC: The National Academies Press.
- Pal I, Nath SK, Shukla K, Pal DK, Raj A, Thingbaijam KKS, Bansal BK. 2008. Earthquake hazard zonation of Sikkim Himalaya using a GIS platform. *Nat Hazards.* 45(3):333–377.

- Pal R, Biswas SS, Mondal B, Pramanik MK. 2016. Landslides and floods in the Tista basin (Darjeeling and Jalpaiguri districts): Historical evidence, causes and consequences. *J Ind Geophys Union*. 2(2): 209–215.
- Patel PP. 2013. GIS techniques for landscape analysis. Proceedings of the State Level Seminar on Geographical Methods in the Appraisal of Landscape; 20 Mar 2012; Kolkata: Dum Dum Motijheel College.
- Patel PP, Sarkar A. 2009. Application of SRTM data in evaluating the morphometric attributes: A case study of the Dulung River Basin. *Pract Geogr*. 38(1):11–12.
- Patel PP, Sarkar A. 2010. Terrain characterization using SRTM data. *J Indian Soc Remote Sens*. 38(1): 11–24.
- Prakash C, Nagarajan R. 2017. Outburst susceptibility assessment of moraine-dammed lakes in Western Himalaya using an analytic hierarchy process. *Earth Surf Process Landforms*. 42(14):2306–2321.
- Quincey DJ, Richardson SD, Luckman A, Lucas RM, Reynolds JM, Hambrey MJ, Glasser NF. 2007. Early recognition of glacial lake hazards in the Himalaya using remote sensing datasets. *Glob Planet Change*. 56(1–2):137–152.
- Racoviteanu A, Arnaud Y, Williams MW, Manley WF. 2015. Spatial patterns in glacier characteristics and area changes from 1962 to 2006 in the Kanchenjunga–Sikkim area, eastern Himalaya. *Cryosphere*. 9(2): 505–523.
- Rai LK, Prasad P, Sharma E. 2000. Conservation threat to some important medicinal plants of the Sikkim Himalaya. *Biol Conserv*. 93(1):27–33.
- Raj BKG, Kumar VK, Remya SN. 2013b. Remote sensing-based inventory of glacial lakes in Sikkim Himalaya: semi-automated approach using satellite data. *Geomatics Nat Hazards Risk*. 4(3):241–253.
- Raj BKG, Remya SN, Kumar VK. 2013a. Remote sensing-based hazard assessment of glacial lakes in Sikkim Himalaya. *Current Sci*. 104(3):359–364.
- Ramakrishnan D, Ghose MK, Vinu Chandran R, Jeyaram A. 2005. Probabilistic techniques, GIS and remote sensing in landslide hazard mitigation: A case study from Sikkim Himalayas, India. *Geocarto Int*. 20(4):53–58.
- Rathore BP. 2018. Mapping, monitoring and modeling of moraine dammed lakes. Training on Satellite based Hydrology & Modeling, 02–11 May, CSD/GHCAG/EPASA/SAC, Ahmedabad. [accessed 2020 Sep 10]. [https://vedas.sac.gov.in/vedas/downloads/ertd/Hydrology/L_18_Glacier_Lakes_Outburst_Flood_\(GLOF\)_Modeling_B_P_Rathore.pdf](https://vedas.sac.gov.in/vedas/downloads/ertd/Hydrology/L_18_Glacier_Lakes_Outburst_Flood_(GLOF)_Modeling_B_P_Rathore.pdf)
- Richardson SD, Reynolds JM. 2000. An overview of glacial hazards in the Himalayas. *Quat Int*. 65–66: 31–47.
- Rounce D, Watson C, McKinney D. 2017. Identification of hazard and risk for glacial lakes in the Nepal Himalaya using satellite imagery from 2000–2015. *Remote Sens*. 9(7):654..
- Rowan AV, Egholm DL, Quincey DJ, Glasser NF. 2015. Modelling the feedbacks between mass balance ice flow and debris transport to predict the response to climate change of debris-covered glaciers in the Himalaya. *Earth Planet Sci Lett*. 430:427–438.
- SAC (Space Application Centre) 2016. ISRO, Ahmedabad (India). Monitoring snow and glaciers of Himalayan region; [accessed 2019 Aug 26]. https://vedas.sac.gov.in/vedas/downloads/SAC_Snow_Glacier_Book.pdf
- Sahana M, Patel PP. 2019. A comparison of frequency ratio and fuzzy logic models for flood susceptibility assessment of the lower Kosi River Basin in India. *Environ Earth Sci*. 78(10):289.
- Salerno F, Thakuri S, D'Agata C, Smiraglia C, Manfredi EC, Viviano G, Tartari G. 2012. Glacial lake distribution in the Mount Everest region: Uncertainty of measurement and conditions of formation. *Glob Planet Change*. 92–93:30–39.
- Sattar A, Goswami A, Kulkarni AV. 2019. Hydrodynamic moraine-breach modeling and outburst flood routing – A hazard assessment of the South Lhonak lake, Sikkim . *Sci Total Environ*. 668:362–378.
- Schwanghart W, Worni R, Huggel C, Stoffel M, Korup O. 2016. Uncertainty in the Himalayan energy–water nexus: Estimating regional exposure to glacial lake outburst floods. *Environ Res Lett*. 11(7): 074005. <http://dx.doi.org/10.1088/1748-9326/11/7/074005>
- Sharma E, Chettri N, Tse-Ring K, Sharma AB, Jing F, Mool P, Eriksson M. 2009. Climate change impacts and vulnerability in the Eastern Himalaya. Kathmandu (Nepal): ICIMOD and MacArthur Foundation; [accessed 2018 Aug 26]. <https://lib.icimod.org/record/26800>
- Sharma LP, Patel N, Ghose MK, Debnath P. 2014. Application of frequency ratio and likelihood ratio model for geo-spatial modelling of landslide hazard vulnerability assessment and zonation: A case study from the Sikkim Himalayas in India. *Geocarto Int*. 29(2):128–146. <http://dx.doi.org/10.1080/10106049.2012.748830>

- Sharma RK, Pradhan P, Sharma NP, Shrestha DG. 2018. Remote sensing and in situ-based assessment of rapidly growing South Lhonak glacial lake in eastern Himalaya. *Nat Hazards*. 93(1):393–409.
- Shrestha DG. 2018. Reducing climate change induced risks and vulnerabilities from Glacial Lake Outburst Flood (GLOF) in South Lhonak Lake in Sikkim. Paper Presented at COP24. Proceedings of the 24th Conference of the Parties to the UN Framework Convention on Climate Change; Dec 2–14; Katowice, Poland.
- Shrestha F, Gao X, Khanal NR, Maharjan SB, Shrestha RB, Wu L, Mool PK, Bajracharya SR. 2017. Decadal glacial changes in the Koshi basin, central Himalaya, from 1997 to 2010, derived from Landsat images. *J Mt Sci*. 14(10):1969–1984.
- Shukla A, Garg PK, Srivastava S. 2018. Evolution of glacial and high-altitude lakes in the Sikkim, Eastern Himalaya over the past four decades (1975–2017). *Front Environ Sci*. 6:81. <http://dx.doi.org/10.3389/fenvs.2018.00081>
- Singh P, Arora M, Goel NK. 2006. Effect of climate change on runoff of a glacierized Himalayan basin. *Hydrol Process*. 20(9):1979–1992.
- Singh P, Kumar N. 1997. Impact assessment of climate change on the hydrological response of a snow and glacier melt runoff dominated Himalayan river. *J Hydrol*. 193(1–4):316–350.
- SSDMA (Sikkim State Disaster Management Authority). 2019. Newsletter. Vol 1, Issue 11. Government of Sikkim. [accessed 2020 Aug 25]. http://www.ssdma.nic.in/Uploads/PdfFiles/issue_II.pdf.
- Strahler S. 1957. Quantitative analysis of watershed geomorphology. *Trans Agu*. 38(6):913–920.
- Sunuwar SC. 2018. Nepal Earthquake 25 April 2015: Hydro projects damaged, risks and lessons learned for design considerations. *J Nepal Geol Soc*. 55(1):141–149.
- Tambe S, Arrawatia ML, Bhutia NT, Swaroop B. 2011. Rapid, cost-effective and high resolution assessment of climate-related vulnerability of rural communities of Sikkim Himalaya. *India Curr Sci*. 101(2): 165–173.
- Thomson N. 2014. Mapping drought for 100 years [Bangalore (India)]: India Water Portal. [accessed 2020 Sep 10]. <https://www.indiawaterportal.org/articles/mapping-drought-100-years>.
- Tsutaki S, Fujita K, Nuimura T, Sakai A, Sugiyama S, Komori J, Tshering P. 2019. Contrasting thinning patterns between lake- and land-terminating glaciers in the Bhutan Himalaya. *Cryosphere*. 13(10): 2733–2750.
- Veh G, Korup O, Roessner S, Walz A. 2018. Detecting Himalayan glacial lake outburst floods from Landsat time series. *Remote Sens Environ*. 207:84–97.
- Veh G, Korup O, Walz A. 2020. Hazard from Himalayan glacier lake outburst floods. *Proc Natl Acad Sci USA*. 117(2):907–912.
- Wang W, Yao T, Gao Y, Yang X, Kattel DB. 2011. A first-order method to identify potentially dangerous glacial lakes in a region of the South-Eastern Tibetan Plateau. *Mountain Res Dev*. 31(2):122–130.
- Wang X, Liu SY, Guo WQ. 2012. Using remote sensing data to quantify changes in glacial lakes in the Chinese Himalaya. *Mt Res Dev*. 32(2):203–212.
- Westoby MJ, Glasser NF, Hambrey MJ, Brasington J, Reynolds JM, Hassan MAAM. 2014. Reconstructing historic Glacial Lake Outburst Floods through numerical modelling and geomorphological assessment: Extreme events in the Himalaya. *Earth Surf Process Landforms*. 39(12):1675–1692.
- Wiltshire AJ. 2014. Climate change implications for the glaciers of the Hindu Kush, Karakoram and Himalayan region. *Cryosphere*. 8(3):941–958.
- Worni R, Huggel C, Stoffel M. 2013. Glacial lakes in the Indian Himalayas: from an area-wide glacial lake inventory to on-site and modelling based risk assessment of critical glacial lakes. *Sci Tot Environ*. 468–469:S71–S84.
- Xu Y, Ramanathan V, Washington WM. 2016. Observed high-altitude warming and snow cover retreat over Tibet and the Himalayas enhanced by black carbon aerosols. *Atmos Chem Phys*. 16(3):1303–1315.
- Yan D, Huang C, Ma N, Zhang Y. 2020. Improved Landsat-based water and snow indices for extracting lake and snow cover/glacier in the Tibetan Plateau. *Water*. 12(5):1339. <http://dx.doi.org/10.3390/w12051339>.
- Yan W, Liu J, Zhang M, Hu L, Chen J. 2017. Outburst flood forecasting by monitoring glacier-dammed lake using satellite images of Karakoram Mountains. *China Quat Int*. 453:24–36.
- Zhang G, Bolch T, Allen S, Linsbauer A, Chen W, Wang W. 2019. Glacial lake evolution and glacier–lake interactions in the Poiqu River basin, central Himalaya, 1964–2017. *J Glaciol*. 65(251):347–365.
- Zhang G, Yao T, Xie H, Wang W, Yang W. 2015. An inventory of glacial lakes in the third Pole region and their changes in response to global warming. *Glob Planet Change*. 131:148–157.
- Zhang M, Chen F, Tian B. 2018. An automated method for glacial lake mapping in High Mountain Asia using Landsat 8 imagery. *J Mt Sci*. 15(1):13–24.

- Zhang M, Wang X, Shi C, Yan D. 2019. Automated glacier extraction index by optimization of Red/SWIR and NIR/SWIR ratio index for glacier mapping using landsat imagery. *Water*. 11(6):1223.<http://dx.doi.org/10.3390/w11061223>.
- Zhao L, Ding R, Moore JC. 2014. Glacier volume and area change by 2050 in high mountain Asia. *Glob Planet Change*. 122:197-207.

Appendix A

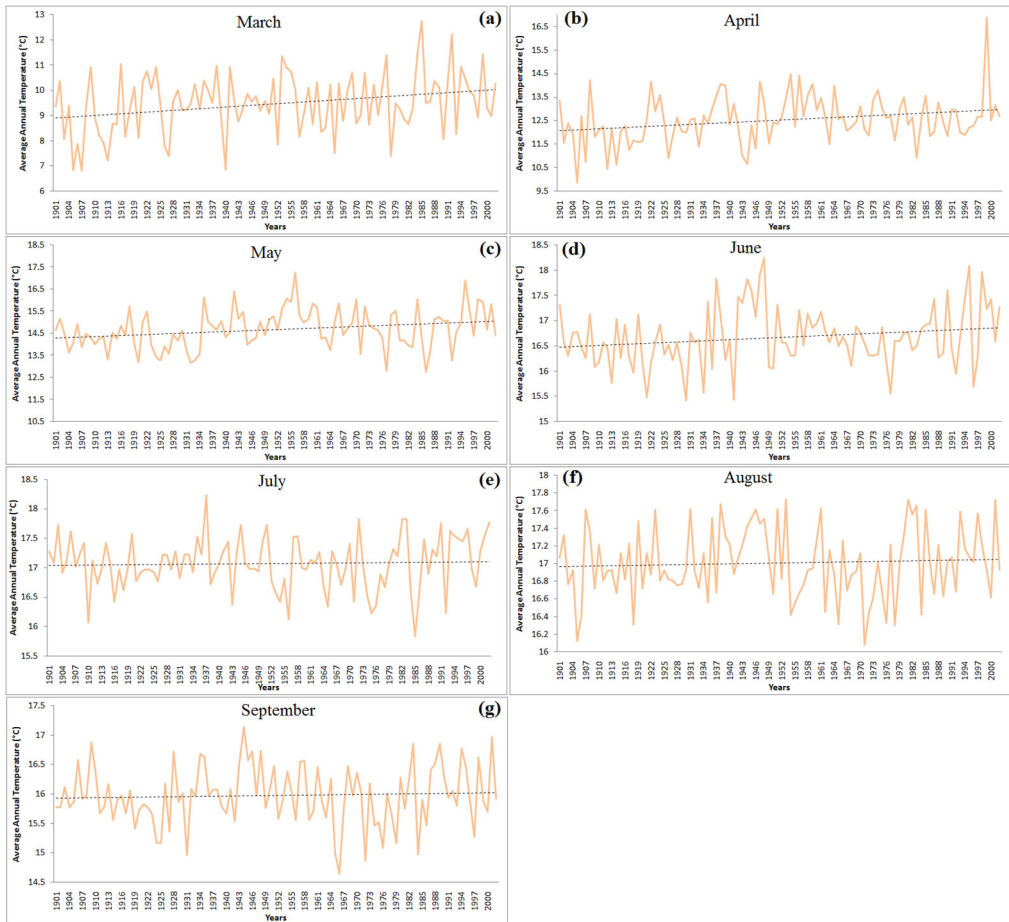


Figure A.1. Temperature trends of the spring and summer monsoon months from 1901 to 2002 (derived from the IMD data for specifically North Sikkim district).

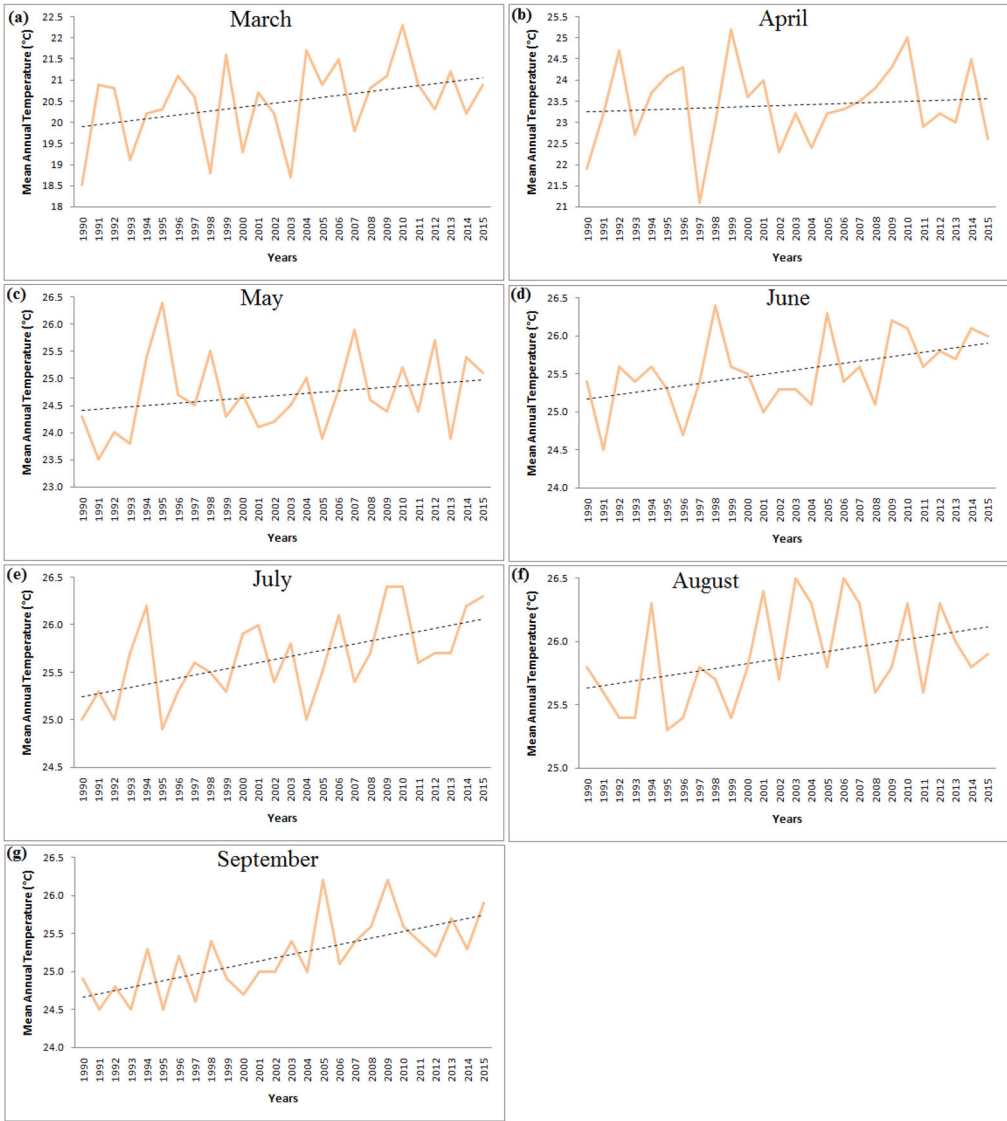


Figure A.2. Temperature trends of the spring and summer monsoon months from 1990 to 2015 (derived from the gridded climate data for Sikkim – tile centroid at 27°50'00"N and 88°50'00"E in North Sikkim district).

Table A.1. Results of Mann-Kendall Test performed on the long-term and short-term temperature datasets used in the study.

Mann-Kendall Test outputs	Long-term (1901–2002) annual average temperature	Long-term (1901–2002) average temperature of warm months (March–June)	Long-term (1901–2002) average temperature of cold months (January, February, November, December)	Short-term (1990–2015) annual average temperature	Short-term (1990–2015) average temperature of warm months (March–June)	Short-term (1990–2015) average temperature of cold months (January, February, November, December)
Kendall's tau	0.363	0.240	0.293	0.327	0.210	0.100
S	1834.000	1214.000	1481.000	94.000	63.000	30.000
Var(S)	116,150.000	116,150.000	116,148.000	1800.667	1832.333	1831.333
<i>p</i> -value (Two-tailed)	< .0001	.00037	< .0001	.028	.148	.498
Alpha	0.05	0.05	0.05	0.05	0.05	0.05

An approximation has been used to compute the *p*-value.

Test interpretation:

H_0 : There is no trend in the series

H_a : There is a trend in the series

If the computed *p*-value is lower than the significance level $\alpha = 0.05$, the null hypothesis H_0 should be rejected and the alternative hypothesis H_a should be accepted.

If the computed *p*-value is greater than the significance level $\alpha = 0.05$, then the null hypothesis H_0 cannot be rejected.

Table A.2. Derived values of Sen's Slope from the Mann-Kendall Test performed on the long-term and short-term temperature datasets used in the study.

Parameters	Long-term (1901–2002) annual average temperature	Long-term (1901–2002) average temperature of warm months (March–June)	Long-term (1901–2002) average temperature of cold months (January, February, November, December)	Short-term (1990–2015) annual average temperature	Short-term (1990–2015) average temperature of warm months (March–June)	Short-term (1990–2015) average temperature of cold months (January, February, November, December)
Slope	0.007	0.008	0.009	0.018	0.020	0.012
Intercept	-1.281	-1.484	-11.206	-14.682	-17.365	-8.437

Significance level (%): 5

Continuity correction: Yes

Confidence interval (%) (Sen's slope): 95

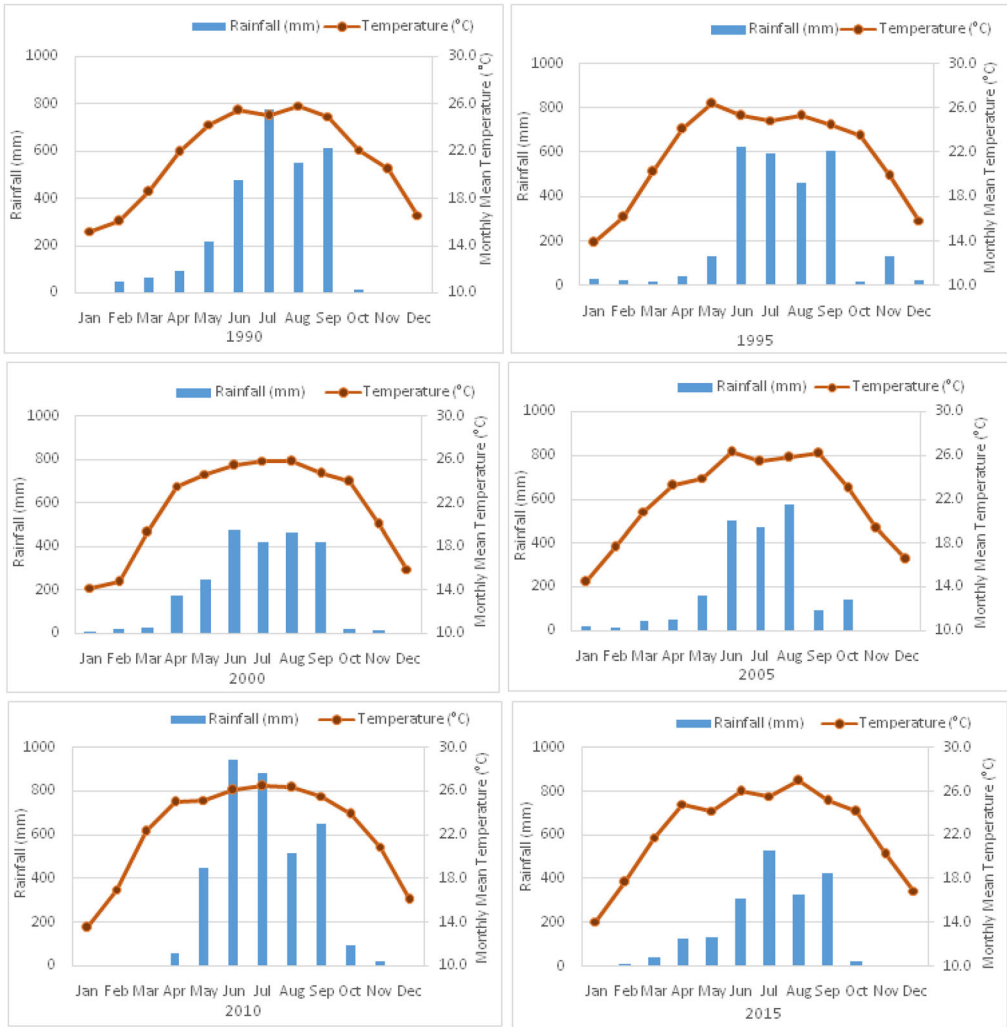


Figure A.3. Monthly variations of temperature and rainfall parameters from 1990 to 2015 at five year intervals (derived from the gridded climate data for Sikkim- tile centroid at 27°50'00"N and 88°50'00"E in North Sikkim district).